TRANSLATIONAL 3D PRINTING; DEVELOPMENT OF AN INTEGRATED STEM CELL ORTHOPEDIC GRAFT PROTOTYPE

KONSTANTINOS MANOS

NATIONAL UNIVERSITY OF SINGAPORE

2017

TRANSLATIONAL 3D PRINTING; DEVELOPMENT OF AN INTEGRATED STEM CELL ORTHOPEDIC GRAFT PROTOTYPE

KONSTANTINOS MANOS

(BSc Biology, MSc Biomedical Engineering)

A THESIS SUBMITTED

FOR THE DEGREE OF MASTER OF SCIENCE

DEPARTMENT OF ORTHOPAEDIC SURGERY

NATIONAL UNIVERSITY OF SINGAPORE

2017

DECLARATION

I hereby declare that the thesis is my original work and it has been written by me in its entirety. I have duly acknowledged all the sources of information which have been used in the thesis.

This thesis has also not been submitted for any degree in any university previously.

KONSTANTINOS MANOS

16 March 2017

Acknowledgements

I would like to thank my supervisor A/Prof Wilson Wang (NUS / Orth. Surgery) for his overall guidance and support, the chairman of my TAC Prof James Goh (NUS / Biomedical Engineering) for his advice and the member of my TAC Dr Yang Zheng (NUS / Orth. Surgery – NUSTEP) for her guidance relative to the stem cell work.

I would like to thank also Dr Michelle Low (NUS / MD2 facilities) for her guidance and support relative to the animal work, Dr Simon Cool (NUS / Orth. Surgery - IMB) for his advice on the experimental design, Mr Muhammed Abdurrahiem Bin Abdul (NUS / Biomedical Engineering) for his help in the 3D printing of the prototypes, Mr Dinesh Parate (NUS / Orth. Surgery - NUSTEP) for his help in the stem cell work, Dr Kingshuk Poddar (NUS / Orth. Susrgery) for his help on the imaging of the prototypes, Dr Glen Liau (NUS / Orth. Surgery) for our meaningful discussions, as well, the MD2 facilities of NUS and all the people there for the kind donation of the freshly sacrificed treatment free rabbits and their support in tissue harvesting.

Finally, I would like to express my appreciation to National University of Singapore and all persons who were involved indirectly in this research project, as well, all my colleagues in the lab for the research conducive and friendly atmosphere.

Table of contents

Summary

Despite the fact that skeletal stem cell tissue engineering (TE) approaches appear promising, these approaches have not yet efficiently translated into large-scale clinical practice. Accordingly, although considerable research has been devoted to the development of stem cell orthopedic grafts, rather less attention has been paid to the optimization of the biofunctionalization of these grafts associated with their regeneration capacity, resulting usually in a random spatial distribution of the cells on the graft and suboptimal diffusion properties. Interpreting the evidence, more integrative studies where multi-factorial experimental settings may closer resemble the in-vivo scenario, might be needed to enhance translational impact and accelerate bridging the gap from bench-to-bedside.

By delivering a high level of tunable control over the microarchitecture of a graft, three dimensional (3D) printing TE technology appears able to extend its scope beyond the control of graft's boundaries, aligned to the rising trend of innovative scaffold designs. Such design-driven optimization studies can serve ideally an integrative developmental framework in the strict context of a clear plan where the effects of the design/geometrical parameters of the graft are not mixed with each other. Taken together as well as the manufacturing limitations of the technology, a respective study towards the optimization of the delicate and dynamic interplay of multiple biofunctionalization factors affected from topological features of the graft at the mesoscale, appears as a well justified research target.

Therefore, following an integrative design-driven optimization approach in the strict context of a clear research plan, this study proposes a novel 3D computer-aided design (CAD) pattern and targets five objectives for the development of the prototype of an integrated 3D printed stem cell orthopedic graft. Additionally, the study isolates a primary adipose-derived stromal/stem cell population and suggests a further developmental pipeline comprised of experiments and respective materials, creating a complete design platform towards the future prototype to product development of the graft.

Relative to the objectives of the study, in terms of commercialization, the minimal size of the CAD pattern appears able to allow the large scale personalized biofabrication of the graft. In terms of biological significance, the biomimetic spatial heterogeneity of the graft appears with potential to control cell positioning on the graft and guide vascularization. Additional "form-follows-function" design micromechanisms in the design/manufacturing interface of 3D printing and microfluidics engineering, appear with potential to develop abilities for 3D cellular aggregation and oxygenation within the pores (artificial stem cell niches) of the graft, so as to maintain cell viability and facilitate the creeping substitution even in the centre of the graft at the early inflammatory stage that vascularization has not yet developed. The overall synergistic effect of the integrated design, especially within non-union clinical cases, is expected to enhance the overall regeneration capacity of the graft in the direction of a functional full-thickness bone healing outcome.

Summarizing, new integrated design-driven optimization approaches not hindered by the limited capabilities of 3D printing technology may be needed

to enhance translational impact in the research field of 3D printing Tissue Engineering (TE). In this context, by developing the prototype of an integrated 3D printed stem cell orthopedic graft according to a clear research plan where the effects of the design/geometrical parameters of the graft are not mixed with each other, this novel study argues the value of the integrated design-driven optimization perspective, triggering the development of a toolkit of microarchitecture-performance relations designed to tailor the large scale personalised biofabrication ability and regeneration capacity of the graft. Additionally, the study isolates a primary adipose-derived stromal/stem cell population and suggests a further developmental pipeline, creating a complete design platform towards the future prototype to product development of the graft.

List of figures

List of symbols and abbreviations

3D	Three Dimensional
ASCs	Adipo-derived Stromal/stem Cells
Bio-CAD	Bio Computer-Aided Design
BMP	Bone Morphogenetic Protein
BMSCs	Bone Marrow Stem Cells
BMSCs	Blood Mesenchymal Stem Cells
CAD	Computer-Aided Design
Col II	Type II collagen
DMED	Dulbecco's Modified Eagle Medium
Egfp	Enhanced Green Fluoresence Protein
EPC	Endothelial Progenitor Cells.
EPR	Electron Paramagnetic Resonance
FBS	Fetal Bovine Serum
FDA	Food and Drug Administration
HA	Hydroxyapatite
HyA	Hyaluronic acid
H&E	Haematoxylin and Eosin
hESCs	Human Embryonic Stem Cells
HIFs	Hypoxia Inducible Factors
hUCMSCs	Human Umbilical Cord Mesenchymal Stem Cells
hiPSCs	Human induced Pluripotent Stem Cells
IACUC	Institutional Animal Care and Use Committee
MSCs	Mesenchymal Stem Cells

p	Partial pressure
PCL	Polycaprolactone
PLLA	Poly-L-lactide
PGA	Polyglycolic zcid
P/S	Penicillin/Streptomycin
RFI	Relative Fluorescence Intensity
SBCs	Spatial Boundary Condition
TGF-β	Transforming Growth Factor beta
TE	Tissue Engineering
VEGF	Vascular Endothelial Growth Factor

Greek symbols

μHM	Micro-Heart Muscle

1. Literature review

1.1. Intro – Clinical need

Bone appears with a remarkable intrinsic property to regenerate and remodel spontaneously, however, it also appears that the critically sized bone defects are not subject to this spontaneous regeneration [1]. In these cases, the host cycle of bone repair appears insufficient and usually respective therapeutic applications require the assistance of bone grafts [2]. Of the millions of bone fractures occurring annually, according to retrospective studies relative to tibial shaft fractures in the U.S.A. [3] and Canada [4], approximately up to 12 % and 18.5 % of cases respectively result in non-union [5]. Thus, a demand appears for more effective clinically applicable bone grafts able to address these cases, with enhanced regeneration capacity and tailored to fit in the fracture area.

1.2. Rationale for more effective solutions (I); Development of optimized stem cell orthopedic grafts

1.2.a. Why a stem cell orthopedic graft

The development of more effective grafts requires a thorough understanding of the bone healing process, especially in cases that bone grafts are used within a respective therapeutic application [1, 2, 5]. Briefly, all types of bone grafts appear to integrate into host bone according to a common mechanism, where the grafts are gradually replaced with host tissue within a process which is called creeping substitution. Capillary networks that sprout

from surrounding tissues grow into the porous structure of the grafts and skeletal stem cells (mesenchymal stem cells "MSCs" or other osteoprogenitor cells) [6] stimulated by osteoinductive biomolecules differentiate into osteoblasts, forming mineralized clusters and producing new mineralized osteoid that is deposited either on the bone matrix, or on some other selected substrate designed for that reason (osteoconductive material). In a later stage, osteoclasts precursors appear to be recruited from the vascular system, where they differentiate so as to facilitate the physiologic remodeling of the graft into mature bone tissue (bone remodeling).

Relative to the MSCs role, the MSCs appear to produce their tissue reparative role in two ways: a) either by contributing directly, differentiating into bone-forming osteoblasts in response to inductive powers and biomolecules, b) or by secreting soluble paracrine factors which target other molecular mechanisms and signalling pathways [7] [8]. The crosstalk between BMP and TGF-β signalling appears as the master regulator towards the differentiation of the MSCs in the osteoblastic lineage [9].

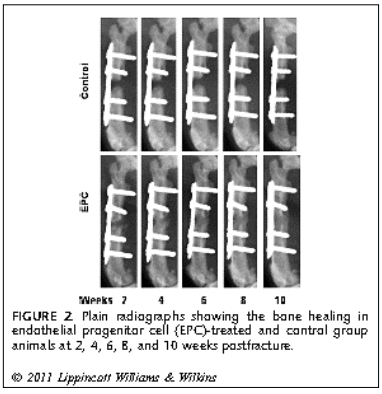

FIGURE 2. Plain radiographs showing the bone healing in endothelial progenitor cell (EPC)-treated and control group animals at 2, 4, 6, 8, and 10 weeks postfracture.

Fig. 1. Photo taken from [14]; bone healing outcome in rat animal model following engraftment of the same bone graft with (*EPC*) and without (*Contro*l) bio-functionalization of the graft with endothelial progenitor cells.

Accordingly, strong evidence which appears as the guiding principle of the majority of the stem cell based TE studies, indicates that by modulating the stem cell niche, someone can modulate the function of stem cell populations driving stem cell

fate [10]. Respective evidence especially within non-union cases [8, 11-13], including striking results (fig. 1) [14], indicates the development of stem cell orthopedic grafts (bone grafts bio-functionalized with stem cells) to enhance the healing process, maximizing the potential for a functional full thickness bone healing outcome.

Escalating the justification for the development of optimized stem cells orthopaedic grafts, these grafts not only appear promising to address effectively non-union cases, but furthermore, evidence supports that one can envisage success within reach within the challenging clinical cases of craniofacial regeneration [15-17].

1.2.b. Appropriate stem cells and stem cell sources; MSCs and ASCs

Back in 1995, the first MSC clinical study used autologous culture-expanded MSCs in patients with hematological malignancies, demonstrated no reports of adverse events. Since this first trial (21 years ago), over 3,000 patients enrolled in over 100 clinical trials have met safety endpoints with no serious adverse events reported to date [18].

More particularly, the potential of stem cells within bone regeneration applications appear well justified and MSCs appear with promising therapeutic potential for bone regeneration applications within animal and pre-clinical studies [8, 19], interestingly even following systemic injection [20]. Within comparative studies including other cell types/populations with MSCs phenotypic expression which potentially can be used within bone regeneration applications (it appears a continuous increase of the stem cell sources that

might be proper for regenerative medicine applications), the comparison between MSCs derived from bone marrow (BMSCs) and MSCs derived from adipose tissue (ASCs) appear conflicting, with some studies to indicate similar osteogenic potential [21]. Other studies, including the comparison of human stem cells from other sources, like umbilical cord (hUCMSCs) and induced pluripotent stem cells (hiPSCs) [22], as well, embryonic stem cells (hESCs) and induced pluripotent stem cells (hiPSCs) [23], suggest that all these stem cells sources/types may be suitable for bone regeneration applications. Highly interestingly, in this direction, stem cell populations with MSCs phenotypic expression derived from amniotic fluid [24], human dental pulp [25] and blood [26, 27], appear able to differentiate towards the osteogenic lineage.

Relative to the justification for the use of ASCs for the purposes of the current study (this study besides the development of a graft prototype, additionally, isolates a primary adipose-derived stromal/stem cell population and suggests a further developmental pipeline, towards the future prototype to product development of the graft), when ASCs are compared with BMSCs (BMSCs are usually used within bone regeneration applications), as mentioned above, ASCs appear also with justified osteogenic potential [11, 28-30]. The major advantage of the ASCs compared to the BMSCs is that they appear abundant within the body and are easy to harvest from adipose tissues, without ethical concerns, following a minimally invasive tissue harvesting process (liposuction). Additionally, another reason for the selection of the ASCs is that evidence supports that they can be obtained without the

limitations of the age-related decline which appears in BMSCs [31] (the "aging" of stem cells appears with less impact on ASCs).

1.2.c. Stem cell orthopedic applications and "Bio-functionalization" of the grafts; Methods and caveats

Despite the well justified evidence and the fact that many orthopaedic surgeons have long appreciated the role of stem cell therapies within small scale clinical applications, these approaches have not yet efficiently translated into a large scale clinical practice [13, 18, 32]. Accordingly, although considerable research has been devoted in the last years to the development of stem cell orthopedic grafts [33, 34], there is rather a paucity of high level of evidenced studies [32], with less attention paid to the optimization of the bio-functionalization of these grafts [35]. Thus, considering as well the natural bone structure (or other organ's structure), where the different types of cells do not appear with a random distribution within the structure, but they appear well organized and aligned to the specific functions of the organ (e.g. osteoblasts forming clusters of mineralization during the osteogenesis progression and endothelial cells forming vasculature), the immersion of a graft in a stem cell hydrogel or the pipetting of stem cell suspensions on a graft by hand, which are the methods that orthopaedic surgeons use most frequently to load ("biofunctionalize") grafts with stem cells, usually these methods result in a random spatial distribution of the cells on the graft [36] and suboptimal diffusion properties of the graft [33]. Accordingly, a recent study [37] which concluded that seeding a TE scaffold with cells using manual

injections appears more effective compared to the dripping protocol, indicates that more efficient respective strategies should be evolved.

Before proceeding with the interpretation of the above contradiction that might lead to some insight able to drive the development of more effective ("optimized") orthopedic grafts, especially within segmental fractures and non-union cases, it is needed to analyse first the usual practice that orthopaedic surgeons apply within these small-scale stem cell clinical therapies and the respective weakness that appears in the application of these therapies. Therefore, orthopaedic surgeons usually prefer to use a graft-stem cell carrier as the optimum solution to carry and localize the stem cells in the targeted fracture area, due to the fact that when the stem cells are mixed with other inductive biomolecules within a biodegradable/biocompatible hydrogel and injected directly in the body in the close vicinity of the fracture area, these injections appear unable to localize the stem cells in the fracture area and maintain their bioactivity (the combination of enzymatic and thermal activity in the fracture area affects negatively stem cells' life span and bioactivity) [38]. But, even when a graft-stem cell carrier is been used to deliver the stem cells, a new caveat arises subject to the random distribution of the cells on the graft and the suboptimal diffusion properties of the graft. A non-uniform bone healing outcome may be developed in these cases, usually with a necrotic center and viable cells forming minimal bone tissue restricted to the graft's boundaries [39]. The poor healing outcome in these cases appear even more challenging towards the need for the development of more effective grafts, especially when considering that cell-cell and cell–extracellular matrix

interactions appear within a highly dynamic microenvironment which provides several opportunities to interfere and drive stem cells' behavior [10], including physical factors which hold key roles in bone development such as blood supply [40] and oxygen content [41].

1.2.d. Scaffolding TE approaches to optimize a stem cell orthopedic graft; Address of bio-functionalization caveats and enhancement of regeneration capacity

Conventional scaffolding TE methods appear currently with limitations in the fabrication of grafts able to answer the above clinical questions of controlling cell position on the graft and regulating the diffusion properties of the graft. Because these methods do not appear efficient to manufacture intricate geometries comprised of well-defined pores, structural integrity and effective interconnectivity between the pores, which are all design elements that appear able to regulate the biofunctionalization ability of the graft so as to address effectively the above issues [42]. Even in grafts fabricated with the newer and highly promising 3D printing TE technology using non cell-laden printing materials [43-45], the cells similarly appear with high difficulty to be seeded efficiently and placed in defined locations on the graft, as the technology appears to have tremendous potential, but still the printing outcome appears similar to the conventional TE techniques (the grafts produced with both TE techniques currently appear with similar properties). On the other hand, when cell-laden bioprinting approaches are used, the high stiffness of the cell-laden bioink which appears as a requirement for enhanced

"printability" (but with a negative impact in the viability of the cells), the generated heat and shear stress on the cells during hydrogel's extrusion (which also appears with a negative impact in the viability of the cells) and the low cells' seeding density of the cell-laden bioink which is suggested (high concentration of the cells in the cell-laden hydrogel appears to block the printing nozzle), all these compromise the efficiency of the highly promising cell-laden bioprinting approach [46]. Subsequently, when an advanced multidispenser extrusion printing system able to print concurrently synthetic polymers and cell-laden hydrogels is being used, one more caveat arises. If a slow cooling after the extrusion polymer has been selected, the viability of the cells in the interface of the cell-laden hydrogel and the slow cooling polymer may be compromised after the extrusion, due to the high temperatures. Thus, as the materials technological progress so far does not allow the selection of the synthetic polymer which will be used for printing within a wide range of materials, a rapid cooling after the extrusion polymer must be selected (the selection of PCL in these cases as a rapid cooling after the extrusion polymer, appears as an optimum material choice [39]).

1.3. Rationale for more effective solutions (II); Integration to enhance translational impact and accelerate translation

Reverting in the interpretation of the gap which appears between experimental and clinical stem cell based TE approaches (bench-to-bedside), in principle, the future of stem cell based TE appears bright. But, considering as well the lengthy/costly clinical trials that are required for the translation of

stem cell research to cell therapeutics [47], more efforts in the preclinical stage aligned to the TE rising trend of biomimetic integrative research strategies [48-50], where multi-factorial experimental settings may closer resemble the in vivo scenario, may be needed to enhance translational impact and accelerate translation. Such integrative strategies use biofabrication techniques which incorporate biomimetic microarchitectures and physical/biochemical elements into a unified customizable manufacturing scheme [39, 48, 50-54].

1.4. Design-driven 3D printing TE; A scaffolding TE technological approach able to merge Rationale I and Rationale II

By delivering a high level of tunable control over the microarchitecture of a graft, 3D printing TE technology can control concurrently many design elements which affect the biofunctionalization ability and subsequently the overall regeneration capacity of a stem cell orthopedic graft. Thus, 3D printing technology appears able to extend its scope beyond the control of scaffold's boundary geometry and serve ideally an integrated developmental research framework aligned to the recent trend of innovative scaffold designs, towards the optimization of the delicate and dynamic interplay of multiple factors affected from spatial features of the inner space of the graft [29, 45, 51].

Four levels of architecture might be considered in such integrative design-driven optimization studies namely surface topography, pore size and geometry, porous networks, and macroscopic pore arrangement, including the potential for spatially varied architectures [55].

These studies and respective CAD modellings [56], may streamline also evidence derived from non-3D printed TE studies relative to microarchitectural geometries which could act as inductive signals, like the porous size [57-59], the porous architecture [60], the design of functionally graded scaffolds (FGSs) where scaffold's pores appear with changes in space according to a specific gradient [61], a microtubule-orientated scaffold with interconnected pores [38] and a microfluidics scaffolding network as structural guiding template within the scaffold for the formation of perfused vasculature [62, 63].

Furthermore, the design-driven optimization research trend appears well established, as current similar studies target innovative scaffold designs with microarchitectures able to optimize the interplay between often conflicting TE elements like biological and mechanical ones [64, 65]. Thus, it appears fair to say that 3D printing TE technology appears as the technology with the highest ability for the development of integrative design-driven optimization studies [44, 66], able to investigate novel geometrical features and new scaffold design concepts, in the strict context always of a clear research plan where the effects of the integrated geometrical parameters of the scaffold/graft are not mixed with each other [42].

Additionally, the unique control engineering ability of the 3D printing technology, appears with a positive impact in the feasibility of an integrative design-driven optimization study. More particularly, the ability of 3D printing technology to deliver a high level of tunable control over the microarchitecture of a graft affecting multiple outputs (microarchitectural geometries which

could have an impact in physical factors), is being coordinated from a single input (CAD/STL file). This single input can be easily and continuously modified by feedback derived from CAD simulations and in-vitro experiments, by simply changing the design parameters of the CAD model. Accordingly, a clearly planned one-pot 3D printing TE study [52, 53] which targets the integrated design of a graft (single input), generates an optimum single-input multiple-output control engineering system able to be modified feasibly and continuously by feedback, towards the optimization of multiple factors that affect the regeneration capacity of the graft.

1.5. A justified research target; Development of the prototype of an integrated 3D printed stem orthopedic graft

Taken together as well the manufacturing limitations of the technology [39, 53, 67, 68] which sets the printing resolution ability at the mesoscale [69], a 3D printing TE study which similar to studies that focus in the computational design of the microarchitecture of a scaffold/graft [70-79], proposes a novel CAD pattern for the 3D printing biofabrication of an integrated stem cell orthopedic graft prototype, creating a design platform towards the further prototype to product development of a graft with ability for large scale personalised biofabrication and enhanced regeneration capacity, appears as a well justified research target. In this context, the "integrated" graft has been developed according to a very clear research plan where the effects of the geometrical parameters of the graft are not mixed with each other. The geometrical parameters of the graft consists of a bio-inspired scaffolding

micro-architecture and concurrently novel “form follows function” design micromechanisms in the design/manufacturing interface of 3D printing and microfluidics engineering. Subsequently, the prototype has been printed within the resolution limitations of the final product/graft, as usually the 3D printers for prototyping appear with higher resolution and manufacturing ability compared to those that they print functional scaffolds/grafts using FDA approved biodegradable/biocompatible materials (these are the materials that the current study suggests for the further prototype to product development of the graft). Finally, as also analysed above, in a manufacturing and clinically “friendly” direction, a non cell-laden 3D printing approach has been selected. This manufacturing approach is expected also to provide more rigidity in the graft, as the frame-added construct would be more effective for supporting its original printed shape compared to a graft comprised only from cell-laden hydrogels. Well justified recent studies [39, 80, 81] which similarly to the current study use polymeric frames, support this manufacturing approach.

2. Hypothesis

The goal of this design-driven optimization 3D printing TE study is to develop the prototype of an integrated stem cell orthopedic graft, through a novel 3D CAD pattern which targets the large scale personalized biofabrication ability and enhanced regeneration capacity of the graft, creating so a design platform for further studies towards the prototype to product development of the graft. The hypothesis is that in terms of commercialization

the minimal pattern size will allow the large scale personalized 3D printing biofabrication of the graft and in terms of biological significance, targeting a toolkit of microarchitecture-performance relations designed to enhance the regeneration capacity of the final integrated product/graft, the graft in the preliminary prototyping stage will appear able to control cell positioning on the graft and develop ability for vascularization, as well, ability for 3D cellular aggregation and oxygenation within the pores (artificial stem cell niches) of the graft.

3. Objectives

Following an integrative design approach in the strict context of a clear research plan, where the effects of the integrated geometrical parameters of the graft are not mixed with each other [42], this design-driven optimization study targets five clear objectives within an one-pot 3D printing manufacturing approach. The above setting targets the development of the prototype of a novel 3D printed integrated stem cell orthopedic graft, through a novel 3D CAD pattern designed to drive the large scale personalized biofabrication and enhanced regeneration capacity of the graft. Due to the limitations of the 3D printing technology, the five objectives have been hierarchically diversified from 1 to 5, based on the increased manufacturing complexity to achieve each one of them, as follows: 1. **Biomimetic design**, 2. **Large scale personalized biofabrication**, 3. **Control of cell positioning on the graft**, 4. **Oxygen supply to the artificial stem cell niches** and 5. **Enhanced regeneration**

capacity. Additionally, this study isolates a primary adipose-derived stromal/stem cell population and suggests a further developmental pipeline, creating a complete design platform towards the future prototype to product development of the graft.

3.1. Objective 1: *Biomimetic design*

Description and mechanism: A biomimetic design of the graft as it is depicted in fig. 4 comprised of two microfluidics networks: a) an osteo-inductive microfluidics network with canals and porous (artificial stem cell niches) as biomimetic template to guide the organized cell positioning on the graft and b) a vascular-inductive microfluidics network as a guiding structural template for the formation of perfused vascular network (please see detailed description in methodology). The biomimetic microfluidics networks within the final model/graft is expected to function as a guiding structural template for the formation of mineralized clusters (MSCs/osteoblast's niches) and perfused vessels similar to the natural bone tissue.

Design rationale: Strong evidence [48, 71, 82-85] suggest a need for biomimetism (the process of simulating what occurs in nature) in TE studies and especially on the development of a vascularization network. Based on these studies, it is not clear to what degree we should mimic natural organs or tissues. However, it is certain that the biomimetic design may include spatial features designed to guide the development of vascular network, cellular

aggregates, nutrients and growth factors at the right time, right position and right amount. A recent review provides an overview of efforts and proposes future perspectives to engineer a functional vascular network [86]. It is needed to highlight also here recent studies where the authors developed pre-vascularized TE scaffolds [1] and microfluidics scaffolding network within a TE scaffold as guiding template for the formation of perfused vasculature together with respective computational models for the optimization of the microarchitecture of the network [62].

More particularly relative to the design rationale for the development of a vascular network, the design approach so as to develop effectively a vascular network for bone regeneration applications, requires insights relative to the role of vascularization on bone regeneration. Thus, inadequate blood supply appears as a significant contributing factor for delayed fracture healing or non-union, with inadequate oxygen supply to appear as the basic causative agent that impairs fracture healing (ischemia occurred often in the fracture area creates a local hypoxic microenvironment, especially within segmental ischemic fractures, which appears to lead in cell death and delayed chondrocyte and osteoblast differentiation) [41].

Also, it appears fair to say that the different origin of the three cell types of skeleton with chondrocytes and osteoblasts derived from the mesenchymal origin and the osteoclasts derived from the monocyte-macrophage cell lineage [7], supports even more the need for a vascularization network able to bring together in the fracture area these distinct cell types. This combination of heterogeneous cells towards the mimic of the complex cellular environment

that occurs during bone healing, might increase the regenerative ability and in situ bone tissue morphogenesis [87].

Experiments as well with non-vitalized TE grafts have shown that the resorption of these grafts depends on the existence of a local functional vascular network. Thus, the development of a functional vascular network may also have a beneficial impact in the biodegradation rate of the graft. [88]

In order to define to what degree we should mimic nature for the development of a vascular network, considering the well justified role of hypoxia inducible factors (HIFs) [89], hypoxic environment appears as a conducive microenvironment for vascularogenesis [41, 88, 90]. A vascular-inductive microenvironment in that case appears inversely related to the local oxygen tension [87, 91, 92]. Therefore, the biomimetic design of a vascular-inductive network within a graft, implies the development of two individual biomimetic microfluidics networks, as following:

a) 1st microfluidics network, an osteo-inductive microfluidics network with canals and porous (artificial stem cell niches) as guiding structural template to guide the organized cell positioning on the graft. The network has been designed to guide the induction of the MSCs to the osteoblastic lineage, targeting the formation of mineralized clusters (osteoblasts' niches), which appears to need exposure to oxygen sources. An oxygen supply design micromechanism in that case, to address the needs for oxygen at the early inflammatory stage that vascularization has not yet developed, especially in the centre of the graft where the development of a functional vascular network appears with more delay, it appears as a well

justified research target (please see in the 4th objective of the current study, the air/oxygen trap design micromechanism).

a) 2nd microfluidics network, a vascular-inductive microfluidics network as guiding structural template for the formation of perfused vascular network (please see detailed description in methodology). The network has been designed to guide the induction of vascularization (perfused vessels), which appears to need hypoxic conditions (the oxygen supply mechanism targets only the 1st microfluidics network).

Taken together, a biomimetic spatial heterogeneity comprised of two individual microfluidics networks, drives the biomimetic design rationale of the 1st objective of the current study (fig. 4). Drawing a conclusion relative to the advantages of such a biomimetic microarchitectural structure of 2 individual microfluidics networks, compared to a homogeneous microarchitecture (e.g. homogeneous lightweight scaffolding structures provided from commercial TE design software programs, carrying repeated parallel or cross motifs), so as to justify furthermore the biomimetic design approach of the current study, it appears to fit ideally to the purposes of this study the suggestion of a recent comprehensive study on bone TE [93], which indicates that when a TE scaffold has been designed for uniform distribution of biologics within the scaffold, this biofabrication approach does not appear optimum for the development of vascularization. Similarly, one more key study, suggests a spatial layering scaffolding technique which drives vascularization in defined areas in the context of VEGF-driven angiogenesis [54].

Therefore, similarly to the biomimetic microarchitecture of the current study, strong evidence indicates that scaffolding microarchitectures which allow spatiotemporal controlled delivery of various inductive factors and cell types, segregating the osteogenic from the vascularogenic signals, may result in improved vascularization outcome.

3.2. Objective 2: *Large scale personalized biofabrication*

Description and mechanism: The minimal pattern unit size (4mmX4mmX3.2mm) as it is depicted in fig. 4 and 6, similarly to the commercial "unit cells" provided from software providers, has been designed to allow easy scaling in the 3D printing biofabrication of the graft (scalable design).

The heterogeneous/biomimetic design novelty of the pattern unit to scale up easily without affecting the integrity of the internal heterogeneous/biomimetic structure of the graft, so as to biofabricate grafts of various sizes homostructural to the lamellar structure of the natural bone and concurrently tailored to fit in any fracture area, is the design mechanism behind the development of ability for large scale personalized biofabrication of the graft.

Design rationale: The lack of heterogeneous/biomimetic "unit cell" patterns within the libraries of software programs like the "Mimics" (Materialise) and "Grasshopper" (Rhino), which can be expanded easily so as

to develop a graft able to fill up with sufficient accuracy the void spaces of fracture gaps, resulted in the innovative idea for the development of an heterogeneous/biomimetic pattern unit ("unit cell").

Therefore, the novelty behind the developed pattern unit ("unit cell") is that it appears with an heterogeneous/biomimetic scalable design compared to the already existed in the market homogeneous ones, which usually are comprised of parallel or crossed repeated motifs.

3.3. Objective 3: *Control of cell positioning on the graft*

Description and mechanism: Similarly to respective microfluidics systems (fig. 2) [94], two "form follows function" design micromechanisms adjusted to the 1st microfluidics network of the graft, designed to control the cell positioning on the final model/graft, as follows:

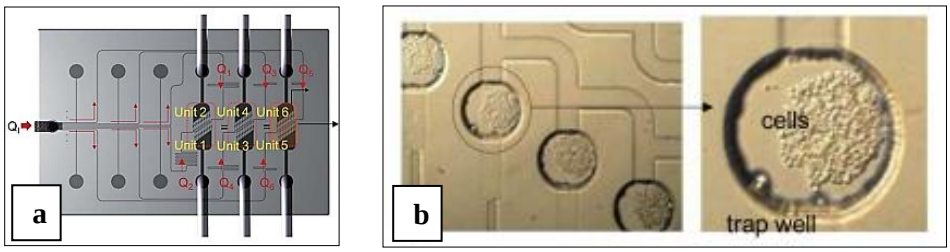

Fig. 2. Photo taken from [94]; microfluidics system with (a) an infusion design mechanism comprised of an inlet tube linked to the microfluidic networks which delivers the cells homogeneously to the network and (b) cell encapsulation technology which develops ability for cell aggregates.

a) An infusion design mechanism comprised of an inlet tube linked to the microfluidics networks of the graft (fig. 2), which is expected to allow the feasible loading of the hydrogels on the graft (for visualization purposes, the

CAD model and the prototypes of the current study, do not include an infusion design mechanism linked to the 2nd microfluidics vascular-inductive network).

b) A cell trap design mechanism as it is depicted in fig. 7 which similarly to existed microfluidics systems (fig. 2b) is comprised of narrow input-output interconnection canals of the porous (artificial stem cell niches). The design mechanism is expected to trap the cells in the pores following the interaction of the spatial configuration with the generated gravitational and fluid forces when the graft is infused with the stem cell hydrogel, developing so ability for 3D cellular aggregation inside the pores.

The combination of the above (a) and (b) mechanisms adjusted to the biomimetic microfluidics network in the final model/graft, is expected to control cell positioning on the graft, guiding the homogeneous distribution of the cells on the graft and concurrently developing ability for forced 3D cellular aggregation inside the pores.

Design rationale: As described also in the literature review part, the manual injection of a scaffold/graft with a stem cell hydrogel, towards the biofucntionalization of the graft with stem cells, appears as a superior approach compared to the dripping protocol. But even though, experimental and clinical results indicate weakness of the technique to drive an homogeneous population of a scaffold/graft with cells. Accordingly, recent studies suggest further research work for the development of scaffolds/grafts with optimized biofunctionalization ability and respective techniques able to address the caveat [37, 95]. In this context, the proposed infusion mechanism

of the current study has been designed so as to address the caveat, driving the homogeneous distribution of the cells on the graft.

Further, MSCs themselves appear to serve as a niche component. Subsequently, 3D MSCs aggregates may improve the therapeutic potential of stem cell applications through increased production of trophic factors, preserved stemness, improvements of ischemia resistance and increased retention and viability in vivo [96] [97] [87]. Respective design strategies targeting stem cells aggregation and cell patterning expanded to the third dimension have been reported also in other studies, targeting a spherical spatial boundary condition (SBCs) as a more conducive microenvironment to induce osteogenesis [98], a more in vivo-like multicellular spheroid structure similar to the structure of the in vivo three-dimensional (3D) stem cell niche [99], a stencil-based strategy to produce micro-Heart Muscle (μHM) arrays the geometry of which drives stem cell's inherent self-organizing capability to generate a uniaxially-stressed substrate-anchored tissue [100] and ASCs cultures in spheroids which appeared with increased therapeutic potential [101].

Taken together the combination of the infusion mechanism linked to the biomimetic microfluidics network and the cell trap design mechanism, the design rationale of the 3rd objective of the current study targets the control of the cell positioning on the graft, providing homogeneous distribution of the cells on the graft and concurrently forced stem cell (MSCs) 3D aggregation inside the pores (artificial stem cell niches) of the graft.

3.4. Objective 4: *Oxygen supply to the artificial stem cell niches*

Description and mechanisms: Similarly to the design rationale of microfluidics systems that provide oxygenation to each well of a cell culture well plate using oxygen control inserts (fig. 3) [102], a "form-follows-function" air/oxygen trap design micromechanism adjusted to the 1st microfluidics network of the graft, comprised of smaller inner space of the pores lower to the height of the interconnection canals, compared to the inner space of the pores above the height of the interconnection canals (unproportional pores design).

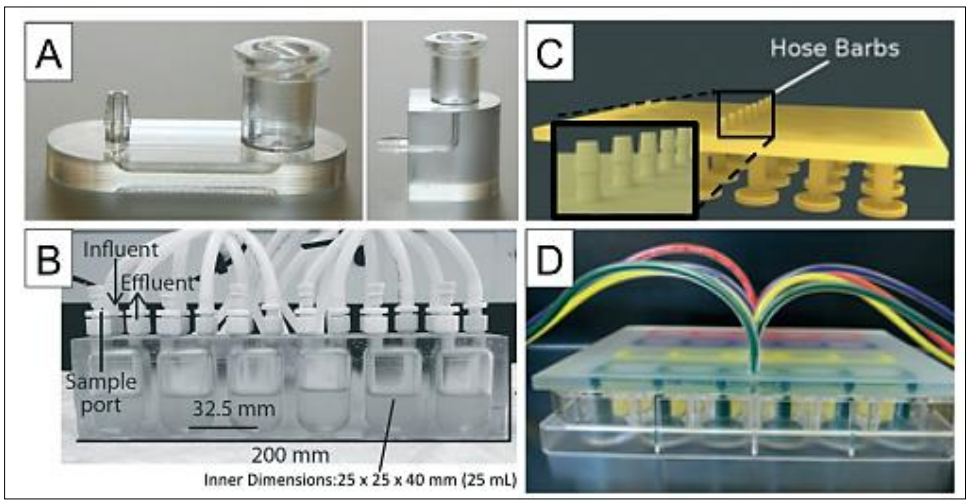

Fig. 3. Photo taken from [102]; microfluidic systems with oxygen control inserts.

The air/oxygen design micromechanism has been designed to trap air/oxygen at the top of each pore, based on the interaction of the spatial configuration as described above with the fluid forces, following the infusion of the graft with the hydrogel (fig. 7). Subsequently, the gelation/solidification of the hydrogel will "lock" the air/oxygen at the top of each pore (the

suggested hydrogel for the further prototype to product development of the graft, is a hydrogel with physical cross-linking ability at 37^{o}C, please see *Chapter 8. - FUTURE STUDIES*). Thus, the stem cells within each pore (artificial stem cell niches) of the graft will have access to air/oxygen so as to maintain cell viability and facilitate the creeping substitution even in the centre of the graft at the early inflammatory stage that vascularization has not yet developed

Design rationale: It is well justified that micro-environmental oxygen tension has an impact on vascularization and fracture healing, so providing locally oxygen in ischemic fractures might lead in an optimized bone healing outcome [41]. More particularly, oxygen as a physical factor and signalling molecule appears to regulate the developmental growth of bone [103] and the fracture healing [41]. Thus, a solution to provide adequate oxygen within hypoxic conditions, appears as a justified research target in stem cell-based TE studies [104].

In such studies, it is considered usually that the vascular damage that occurs within large bone injury, renders sites of bone defects ischemic. Delivering stem cells to the defect site within a stem cell based therapeutic approach, increases further the local metabolic demand and worsens the detrimental effects arising from the lack of adequate oxygen supply, as functional vascularization of a bulky orthopaedic graft may take weeks. Hence, in stem cell-based TE approaches, maintaining cell viability within this harsh

environment (absence of a functional vascular network), it appears as an imperative challenge.

Respective studies suggest further investigation for more efficient strategies to maintain cell viability, mainly due to diffusion which appears as the primary mechanism in these cases for delivering oxygen and nutrients to the cells [37, 95]. Subsequently, within conventional stem cell TE scaffolds/grafts, many cells/tissues suffer from hypoxia and/or deprivation of nutrients, because it is well established that the diffusion length of oxygen and the maximum respective diffusion distance for cells seeded in a scaffold/graft as to survive in the absence of a functional vascular network, is less than 200 μm. So, the central area of engineered tissues greater than 1 cm^3 appears often hypoxic, resulting subsequently in imperfect tissues with a necrotic center and viable cells forming minimal tissue restricted to the graft's boundaries. Thus, it is suggested that the cells must be localized within the indicated distance of the 200 μm from oxygen sources, to prevent hypoxia and necrosis [39, 85, 105].

In aggregate, a design-driven optimization rationale for the development of novel scaffolds/grafts with enhanced "biofunctionalization" ability which will lead in more efficient seeding techniques, where the scaffolds -among others- will appear with enhanced diffusivity [106] and the cells will be able to withstand the oncoming hypoxic insult until new vessels have formed [37], appears as a justified design rationale. A well justified recent study verifies the design rationale of the current objective, targeting to ensure effective transport oxygen and nutrients to encapsulated cells within a microfluidics system [107].

Accordingly, the proposed air/oxygen design micromechanism which constitutes the 4th objective of the current study, targets to provide adequate oxygen supply in the stem cells following the entrapment of air/oxygen at the top of each pore of the graft..

3.5. Objective 5: *Enhanced regeneration capacity*

Description and mechanism: The synergistic effect of all the objectives of the current study is expected to affect beneficially the overall regeneration capacity of the graft, within future studies towards the further prototype to product development of the graft.

Design rationale: All integrated studies described above target a beneficial synergistic effect based on the multi-factorial experimental setting of each study.

4. Scientific significance

By developing the prototype of an integrated 3D printed stem cell orthopedic graft, this novel study triggers the development of a toolkit of microarchitecture-performance relations designed to tailor the large scale personalised biofabrication ability and regeneration capacity of a graft. In terms of biological significance, the biomimetic spatial heterogeneity of the graft in the prototyping stage appeared with potential to control cell

positioning on the graft and guide vascularization. Additional "form-follows-function" design micromechanisms in the design/manufacturing interface of 3D printing and microfluidics engineering, appeared also with potential to develop ability for 3D cellular aggregation and oxygenation within the pores (artificial stem cell niches) of the graft, so as to maintain cell viability and facilitate the creeping substitution even in the centre of the graft at the early inflammatory stage that vascularization has not yet developed. The overall synergistic effect of the integrated design, especially within non-union clinical cases, is expected to enhance the overall regeneration capacity of the graft in the direction of a functional full-thickness bone healing outcome. Additionally, the study isolates a primary adipose-derived stromal/stem cell population and suggests a further developmental pipeline towards the further prototype to product development of the graft.

5. Methodology

5.1. Design methodology

Despite the fact that the microarchitecture of a graft appears to affect graft's regeneration capacity, so as the design-driven optimization of the microarchitecture of a graft to be a justified research target [55, 61, 64, 65, 108, 109], a single optimal microarchitecture does not exist. Microarchitectural optimized structures may be developed only on a case-by-case basis and accordingly to individual fracture-specific features [55]. Also, the link

between grafts' microarchitecture and stem cell behavior is still far from being completely understood, so progress in the quantitative microarchitectural description of TE scaffolds is needed for the identification of the optimum graft microarchitecture, getting closer to design-driven optimized grafts [109].

Accordingly, defining the optimal design for an integrated stem cell orthopedic graft, appropriate for transplantation and able to drive bone regeneration, is a complex process. In such studies, determination of the key factors affected from the microarchitecture design that appear to influence the regeneration capacity of the graft is being required. Design ideas and design mechanisms derived from biological systems or man-made devices, including microfluidics systems with cell encapsulation technology (fig. 2) [94], microfluidics systems within semienclosed space with multiple inlets [107] and "revolutionary" 3D printed microfluidics systems [102] that introduce oxygen control systems (fig. 3) [102] [110], could be also useful in such studies.

More particularly, working on the design/manufacturing interface of the microfluidics systems and 3D printing TE technology, some of these microfluidics ideas, by compromising the structural integrity of the final graft, may be translated from the microfluidics to 3D printed scaffolds/grafts. Aligned to this rationale, this study targets "form-follows-function" microarchitecture design configurations of microfluidics systems which in addition with other variables that affect the flow rate, they have designed to allow the control of cell positioning on the system and to provide oxygen to the cells. A recent well justified study where they combined the direct 3D-

printing of cell-laden constructs in microfluidic microarchitectures [111], is strongly indicative of the highly promising interplay between the 3D printing microfluidics engineering and 3D printing TE scaffolding biofabrication.

Highly importantly also and as the aim of the current study is to develop the prototype of a novel graft so as to set the basis for future studies for the further development of the graft, it is needed to highlight here that despite the fact that the prototype has been printed with a commercial 3D printing system (Stratasys - Objet260 Connex1) and a respective proprietary 3D printing material (Stratasys - RGD720 transparent material) that provides relatively high resolution manufacturing ability >30 μm, the CAD model and the respective prototype outcome has been adjusted to the requirements and manufacturing limitations of the technology for printing biodegradable and biocompatible materials with an open extrusion/jet 3D printing system (this is the system that this study suggests for the future development of the graft), which implies orthogonal configuration in the design of the porous/canals and relatively low resolution ability > 200 μm.

Therefore, an integrative design approach in the strict context of a clear research plan where the effects of the integrated geometrical parameters of the graft at the mesoscale (resolution >200 μm) are not mixed with each other [42], including literature evidence that suggests microarchitectural geometries and topological features conducive for TE bone regeneration applications, as well engineering inspiration derived from microfluidics systems, the lamellar structure of the natural bone and “form-follows-function” architectural

solutions for bioclimatic constructions, resulted in the development of the CAD model of the current study (fig. 4) and the respective prototype (fig. 6).

5.2. CAD model

The CAD model (fig. 4) of the pattern unit which for the reasons that analyzed extensively above incorporates two individual microfluidics networks within an all-in-one minimal pattern unit of 4mmX4mmX3.2mm, is comprised of the following quantitative microarchitectural design elements:

1st microfluidic network (osteoinductive hydrogel): *Infusion mechanism*: Tube with 1 mm diameter which is linked to all infusion canals of the 1st microfluidic network. *Infusion canal* ("haversian" canal): "large" square canal (side of 1 mm) designed for high permeability as to avoid as much as possible the generation of shear stress on the cells and clogging effects during the infusion of the stem cell hydrogel on the graft, and subsequently, as to deliver homogeneously and with a consistent flow rate the stem cells even in the deepest areas of the graft, where there the cells will be distributed to all interconnection canal-porous canals of the graft. *Exit canal* ("haversian" canal): the same boundaries with the entry infusion canal but with different design rational, as in this canal there is no need for consistent flow rate, so a cross grid configuration has been added in the inner space of the canal designed to provide macroscale spatial features for the cells to adhere. *Porous* (artificial stem cell niches): according to the literature for optimum osteogenicity which implies a graft with side pore size between 300 μm -

800 μm [42, 57, 112] and considering as well the manufacturing limitations of the 3D printing technology, the pore has been designed with the dimensions of 0.5mmX0.5mmX0.8mm. As analyzed in the objectives, the unproportional design of the pores relative to the interconnected canals, is expected to render porous as cell and air/oxygen trap mechanisms. *Canal-porous and porous-porous interconnection canals* ("canaliculus"): these canals appear with the highest manufacturing difficulty as they have been designed with a side of 0.2 mm which appears close to the resolution limitations of the suggested technology for the future prototype to product development of the graft (>0.2 mm).

2nd microfluidic network (vascular-inductive hydrogel): *Infusion mechanism*: Tube with 1 mm diameter identical to the infusion mechanism of the 1st microfluidic network, which is linked to the 2nd microfluidic network. For visualization purposes this second infusion mechanism is not included in the CAD model and the prototypes. *Perforatory canals* ("Volkman's canal"): "Large" vertical canal (side of 1 mm) connected to the 2nd microfluidic network which as analyzed extensively in the objectives, it is expected to guide the formation of perfused vessels.

5.3. CAD model evaluation - Computational flow simulation

Computational flow simulation (SOLIDWORKS) has been applied in the CAD model of the pattern unit for the evaluation of the osteo-inductive flow path (1st microfluidics network) and the respective diffusion properties of the

unit. The experimental setting and the results are described in the *materials* and in fig. 5. For the 2nd microfluidics network at the current developmental stage of the prototype there is no need for computational flow simulation, as this network is comprised of simple linear canals, so the respective flow simulation as applied in the 1st microfluidics system, will not provide any useful information.

5.4. Prototype model

Three prototype models were printed as follows:

a) Actual size visual prototype of the unit pattern. Considering as well the non-dissolvable properties of the supporting printing material which was used for the 3D printing of the prototype, the supporting material has remained within the graft to visualize the loading hydrogels (fig. 6).

b) Scaled up X10 visual prototype of the unit pattern. Considering as well the non-dissolvable properties of the supporting printing material which was used for the 3D printing of the prototype, the supporting printing material has remained within the graft to visualize the loading hydrogels (fig. 6).

c) Scaled up X25 functional prototype of the oxygen trap design mechanism where the supporting material has been removed (the X25 scaled up model of the prototype allowed the extraction of the supporting printing material, by scratching the material with a pair of

forceps), so as to proceed further with an experimental flow simulation test (fig. 7).

In the future prototype to product developmental studies of the graft which are suggested in details below (please see *Chapter 8. FUTURE STUDIES*), biodegradable/biocompatible 3D printing materials and dissolvable 3D printing supporting materials it is expected to allow the extraction of the supporting material from the graft, so as to proceed with the suggested evaluation tests using cell-laden hydrogels.

5.5. Prototype morphology characterization - Evaluation of CAD to prototype model transition

Top, bottom and side view images of the CAD model, the actual size visual prototype and the scaled up 10X prototype used for the morphological characterization (shape, structure and visualization of flow path) of the prototype models and the respective evaluation of the transition from the CAD model to structure (fig. 6).

5.6. Prototype model evaluation - Experimental flow simulation

Experimental flow simulation applied in the scaled up X25 functional prototype model of the oxygen trap design mechanism for the evaluation of the mechanism. The experimental setting and the results are described in fig. 7.

5.7. Isolation of adipose derived stromal/stem cells

White abdominal adipose tissue was harvested from freshly sacrificed rabbits in the MD2 animal facilities of NUS, using aseptic techniques. Following respective protocol where is described in details the procedure and concentrations of the reagents used [113], the adipose tissue was proceeded further for the isolation of adipose derived stromal/stem cells.

Briefly the protocol, the adipose tissue was minced into small pieces using sterilized scissors, washed with equal volumes of warm PBS containing EDTA, FBS and P/S, to remove blood cells and subsequently digested with collagenase type I with intermittent shaking at 37 ^{o}C for 60 min. The enzyme activity was terminated by dilution with DMEM containing FBS and the floating adipocytes were separated from the stromal cell fraction by adding slowly Ficol-Paque® and centrifugation at 300g for 25 min. The cells aspirated from the middle layer of the formed layers in the tube and incubated overnight at 37 ^{o}C with 5% CO2 in MSCs culture medium containing DMEM, Glutamax, FBS and P/S. The isolated primary cells were cultured in T175 flasks until they reached confluence and defined as passage zero. The nonadherent cells were removed 5 days after plating and the adherent cells allowed to proliferate in the expansion media until they reached 90% confluence. The confluent cells were subcultured up to passage 2 and the expansion MSCs medium was replaced every 3-4 days, so as after a cell culture of 3 weeks, to collect 4.22 X10^{6} adipose derived stromal cell which can be used within future studies for the prototype to product development of the

graft (the cells cryopreserved in cryosolution and cryovials with $2X10^5$ cells in each vial). The rest of the cells devided in three groups and proceeded for cell characterization according to a three lineages differentiation test [114, 115] which required 21 days of cell culture and differentiation induction.

5.8. Differentiation induction of primary adipose derived stromal/stem cells

Following respective protocol aligned to the three lineage differentiation test, where is described in details the procedure and the concentrations of the reagents used [114], the isolated cells devided into three differentiation induction cell culture groups and respective control groups. Following, the cells proceeded for 21 days of osteogenic, adipogenic and chondrogenic cell culture differentiation induction and subsequent histological and immunohistochemical analysis. The group 1 and 2 cultured in 24-well tissue culture plates according to osteogenic and adipogenic differentiation induction protocols respectively and the 3rd group cultured in 15 ml polypropylene screw-cap tubes where the cells were pelleted to form a 3D cell aggregate according to the chondrogenic differentiation induction protocol. Briefly the protocols:

1st group - osteogenic induction: The isolated cells were plated at a density of 3×10^4 cells/cm^2 on a 24-well tissue culture plate in MSC expansion media containing low glucose DMEM, FBS, P/S and Glutamax and allowed to adhere overnight at 37°C. The osteogenic differentiation induced by replacing

the MSC expansion medium with osteogenic media consisting of low glucose DMEM, FBS, dexamethasone, ascorbic acid, b-glycerophosphate, MEM sodium pyruvate, P/S and Glutamax. The control group of the cells was plated and maintained only in the MSC expansion media and all medium changed every 3 days for a period of 21 days.

2nd group - adipogenic induction: The isolated cells were plated at a density of 6×10^4 cells/cm^2 on a 24-well tissue culture plate in MSC expansion media containing low glucose DMEM, FBS, P/S and Glutamax and allowed to adhere overnight at 37°C. The adipogenic differentiation induced by replacing the MSC expansion medium with adipogenic media consisting of high glucose DMEM, FBS, P/S, Glutamax, insulin, isobutylmethylxanthine, sodium pyruvate, dexamethasone and indomethacin. Similarly to the osteo-inductive protocol, the control group was plated and maintained only in the MSC expansion media and all medium changed every 3 days for a period of 21 days.

3rd group - chondrogenic induction: A cell density of 5×10^5 cells / ml was used and the cell pellets formed by aliquoting 0.5 ml of cell suspension into each 15 ml polypropylene screw-cap tube and subsequent centrifugation at 300×g for 5 min. The control cell culture medium consisted of high glucose DMEM, dexamethasone, L-proline, ascorbic acid, ITS+Premix, MEM sodium pyruvate, Glutamax and P/S. For the chondrogenic differentiation medium, the TGFb3 growth factor added in the control medium. Three pellets were prepared for each group and the caps of the tubes were loosen during the incubation period in a 37°C incubator with 5% CO_2 as to allow air exchange. The media was replaced every 2 days for a period of 21 days.

5.9. Characterization of primary adipose derived stromal/stem cell plasticity using morphological features - Optical microscopy, histological and immunohistological staining

Following respective protocols aligned to the evaluation of the three lineage differentiation test [114, 115], after 21 days of cell culture, the cells were collected and proceeded for the evaluation of their plasticity, using morphological analysis of optical microscope images taken following the histological and histo-morphological staining of the cells. The results together with a brief description of the protocols are described in fig. 8 and 9 (please see *results*).

6. Materials

CAD Model: The CAD models of the prototype and the respective STL files have been developed with the SOLIDWORKS and AUTODESK 123D DESIGN software programs. **Prototype model:** The prototype models have been printed using a Stratasys-Objet260 Connex1 3D printer and the respective RGD720 transparent material (Stratasys). **Flow simulations:** DMEM (Gibco/Invitrogen) cell culture medium was used in the experimental flow simulation and "water" in the computational one. **Imaging:** The images of the prototypes have been taken with an Olympus camera. **Tissue harvesting – animal models:** Two treatment-free freshly sacrificed New Zealand male rabbits were kindly donated from the MD2 animal facilities of

NUS for the adipose tissue harvesting. **Stromal/stem cell isolation, culture and differentiation induction:** *Stromal/stem cells isolation:* DMEM (Gibco/Invitrogen), FBS (Gibco/Invitrogen), GlutaMax-I Supplement (Gibco/Invitrogen), P/S (Gibco/ Invitrogen), TrypLE™ Express Stable Trypsin-Like Enzyme with Phenol Red (Gibco/Invitrogen), Ficol-Paque® (GE Healthcare). *Osteogenic induction:* DMEM low-glucose (Gibco/Invitrogen), FBS (Gibco/Invitrogen), GlutaMax-I Supplement (Gibco/Invitrogen), P/S (Gibco/ Invitrogen), Sodium pyruvate (Gibco/Invitrogen), ascorbic acid (Sigma), Dexamethasone (Sigma), b-glycerol phosphate disodium salt pentahydrate (Sigma). *Adipogenic induction:* DMEM high-glucose (4.5 g/L; Sigma), FBS (Gibco/Invitrogen), GlutaMax-I Supplement (Gibco/Invitrogen), P/S (Gibco/Invitrogen), Dexamethasone (Sigma), Insulin (Gibco/Invitrogen), Isobutylmethylxanthine (GMCN; Calbiochem/Merck), Indomethacin (Sigma). *Chondrogenic induction:* DMEM high-glucose (4.5 g/L; Sigma), GlutaMax-I Supplement (Gibco/Invitrogen), P/S (Gibco/Invitrogen), Sodium pyruvate (Gibco/Invitrogen), ITS+1 (BD Bioscience), Ascorbic (Sigma), L-Proline (Sigma), Dexamethasone (Sigma), Recombinant human transforming growth factor-beta3 (TGFb3) (R&D Systems). **Stromal/stem cell histological and immunohistochemical evaluation**: *Osteogenic direction - Alizarin red staining:* Formalin (Sigma), Alizarin red S (Sigma), Ammonium hydroxide (Sigma), Dulbecco's Ca2+- and Mg2+-free phosphate-buffered saline (First Base). *Adipogenic direction - oil red O staining:* Oil Red O (Sigma), Hematoxylin (Sigma). *Chondrogenic direction - fixation and paraffin processing:* Formalin (Sigma), Eosin Y (Sigma), Xylene (VWR, International

S.A.S), Paraffin wax (Leica Biosystems), embedding machine (EG1160, Leica Biosystems), microtome (RM2135, Leica Biosystems). *Hematoxylin and Eosin Staining:* Hematoxylin (Sigma), Eosin Y (Sigma), Scott's tap water (Sigma). *Proteoglycan deposition - safranin O:* Fast green (Sigma), Safranin O (Acros Organics). *Collagen deposition - immunohistochemical detection:* UltraVision HRP Detection System (Lab Vision Inc.) containing Ultra V Block, Biotinylated Goat Antimouse IgG, Streptavidin Peroxidase, Diaminobenzidine (DAB) substrate, and DAB Chromogen, Pepsin (Lab Vision), Hydrogen peroxide block (Lab Vision), Monoclonal anticollagen type II, clone II-II6B3 (Chemicon Inc.), Control mouse IgG isotype (Invitrogen).

7. Results

7.1. CAD model – biomimetic scalable design

The biomimetic and scalable CAD model captured and developed for the purposes of the 1st and 2nd objective of this study is depicted in the following fig. 4. As analysed extensively above, the heterogeneous/biomimetic minimal pattern unit size (4mmX4mmX3.2mm) which incorporates two individual microfluidics networks (osteo-inductive network with canals and porous and vascular-inductive network only with canals), allows easy scaling towards the 3D printing biofabrication of the graft (scalable design), without affecting the integrity of the internal heterogeneous/biomimetic structure of the graft

(currently in the market are only provided homogeneous “unit cells”, comprised usually of parallel or crossed repeated motifs) .

Therefore, the novel 3D CAD pattern unit depicted here appears able to allow the future large scale personalized 3D printing biofabrication of the graft, as well, it provides a structural guiding template to control cell positioning on the graft and guide vascularization, towards the further prototype to product development of the graft.

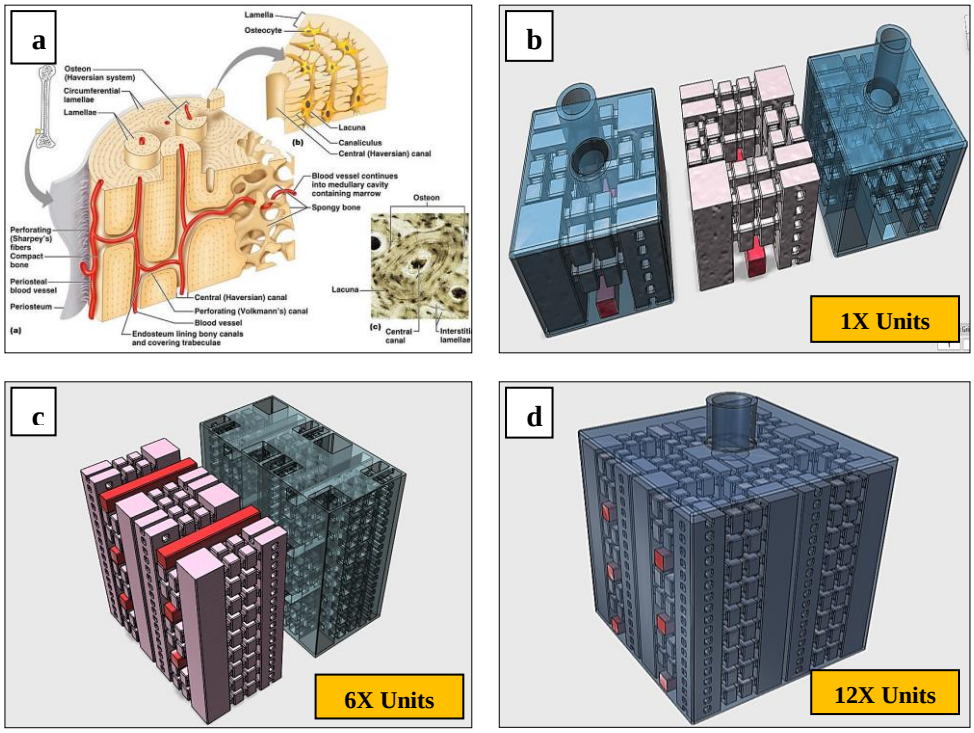

Fig. 4. Biomimetic scalable design. (a) Microscopic view of the lamellar structure of the natural cortical bone (http://classes.midlandstech.edu/carterp/Courses/bio210/chap06/lecture1.html) and (b, c, d) respective biomimetic CAD models of various sizes of the graft (blue-green transparent colour) where is depicted the biomimetic design of the graft (haversian system, volkmann’s canals, canaliculus and osteoblasts’ mineralized niches), the infusion design mechanism (inlet tube) linked to the artificial stem cell niches hydrogel and the visualization of the 2 individual microfluidics networks designed to guide the infusion of the osteo-inductive (pink opaque colour) and vascular-inductive (red opaque colour) loading hydrogels; (b) From left to right: (i) 1X unit graft (pattern unit) loaded with both hydrogels, ii) visualization of both loading hydrogels and iii) 1X unit graft, (c) From left to right: i) visualization of both loading hydrogels in a 6X units graft and ii) the 6X units graft without the infusion mechanism (tube) for a clearer top view, (c) 12X units graft loaded with both hydrogels.

7.2. Computational flow simulation – proof of concept for the flow path and the cellular and oxygen trap design mechanisms

The computational flow simulation test of the current study (fig. 5b) appears as a proof of concept evidence for the developed CAD model and respective prototype, as it verifies the design rationale behind the flow path and the diffusion properties of the graft.

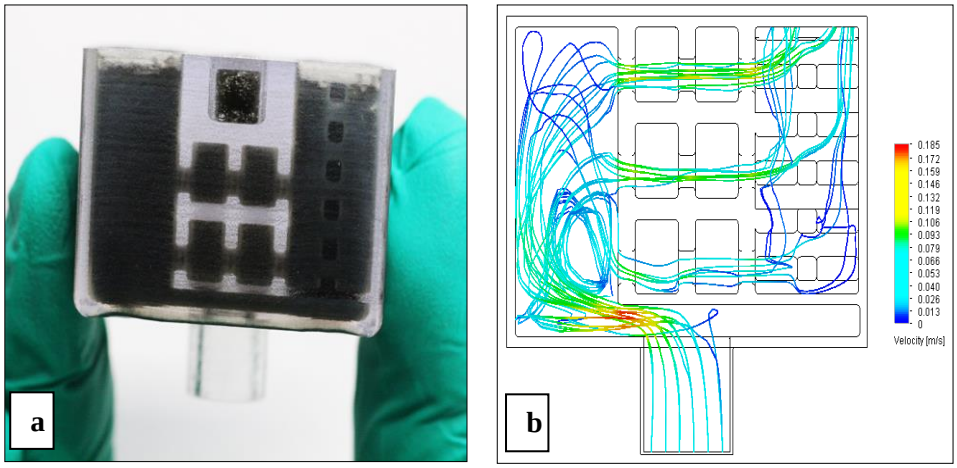

Fig. 5. Proof of concept for the flow path and the cellular and oxygen trap design mechanisms based on computational flow simulation; (a) Scale (human fingers) and high contrast photo of the 10X scaled up visual prototype of the pattern unit (transparent material) loaded with the supporting 3D printing material (opaque material) which visualizes the flow path of the loading hydrogels. (b) Computer screen photo of the computational flow simulation of the pattern unit (continuous flow all over the graft with white spots on the top of each pore and condensed flow in the centre of the pores).

More particularly, the computational flow simulation (fig. 5b) appears continuous and aligned to the flow path of the prototype (fig. 5a), with homogeneous distribution of the flow chart (hydrogel) to all interconnected canals/pores, white colour areas at the top of the pore where is expected the entrapment of air/oxygen bubbles (air/oxygen trap design micromechanism)

and condensed flow in the centre of each pore where is expected the 3D cellular aggregation (cell-trap design micromechanism).

Therefore, similarly to the technology in microfluidics which develop systems able to encapsulate cells and provides air/oxygen at the top of each well in a cell culture plate (fig. 2 and 3), it appears with potential the entrapment of cells and air/oxygen inside the pores, developing so ability for 3D cellular aggregation and oxygenation within the pores (artificial stem cell niches) of the graft.

7.3. Prototypes - evaluation of the transition from CAD model to structure

In respective photos within fig. 6 from the top view (a, d, g), bottom view (b, e, h) and side view (c, f, i) of the 3D printing outcome-transition from CAD model to structure (left to right), the generated visual prototypes appeared with a good level of agreement compared to the CAD model, especially relatively to the intricate manufacturing details of the narrow interconnected canals and the unproportionally shaped porous which develop the cell and air/oxygen design micromechanisms (e, f, h, i).

As it was expected, between the 10X scaled up pattern unit visual prototype and the actual size visual prototype, the scaled up prototype appears with a more consistent structural integrity and uniform flow path. The results appear encouraging for future studies for the further prototype to product development of the graft, where is expected a lower level of agreement

between the CAD model and the final model/graft (with the current available technology, lower resolution ability it is expected when will be used the 3D printing systems / materials that the current study suggests for the further prototype to product development of the graft).

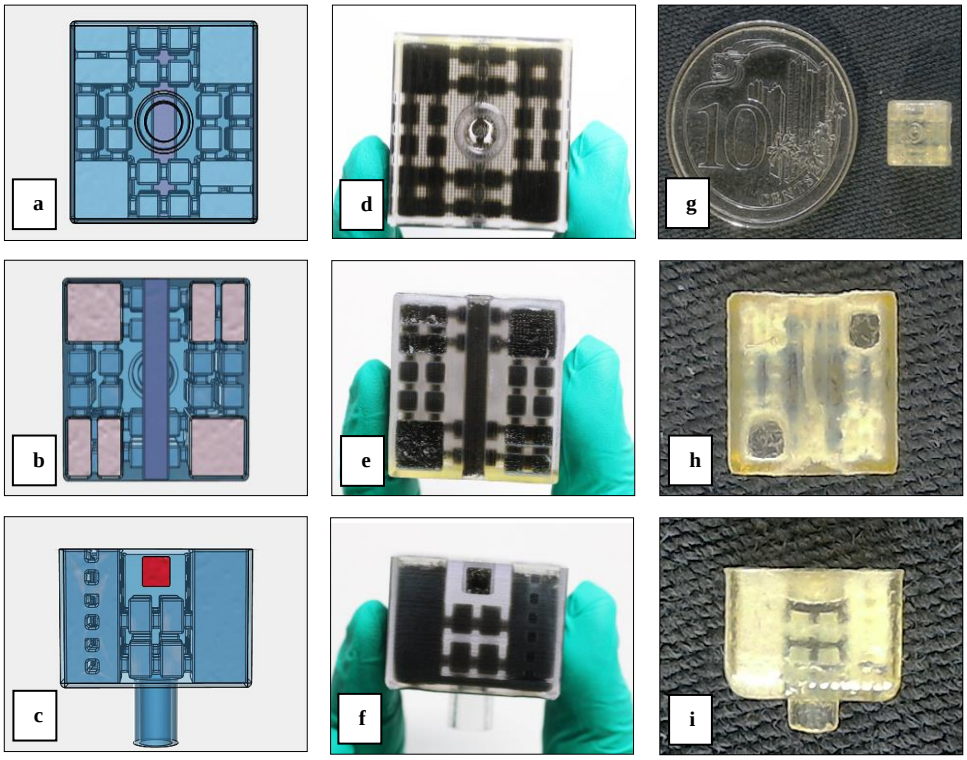

Fig. 6. Evaluation of the transition from CAD model to structure. Optical comparison of the CAD model of the X1 unit graft (pattern unit) with the respective actual size and X10 scaled up visual prototypes; (a, b, c) CAD model of the pattern unit (transparent blue colour) loaded with the 2 types of hydrogels where the flow path of the osteogenic stem cell hydrogel has been visualized with pink opaque colour and the vascularization hydrogel with red colour, (d, e, f) photos with scale (human fingers) and the 10X scaled up visual prototype of the pattern unit (transparent material) where the supporting 3D printing material (opaque black material) visualizes the flow path of the loading hydrogels, (g) photo with scale bar (10 cents coin) and the actual size visual prototype of the pattern unit, (h, i) magnified detailed photos of the actual size visual prototype of the pattern unit (transparent material) where the supporting 3D printing material (opaque pale white material) visualizes the flow path of the loading hydrogels.

7.4. Experimental flow simulation - Proof of concept for the oxygen trap design mechanism

The experimental flow simulation test of the current study (fig. 7), appears

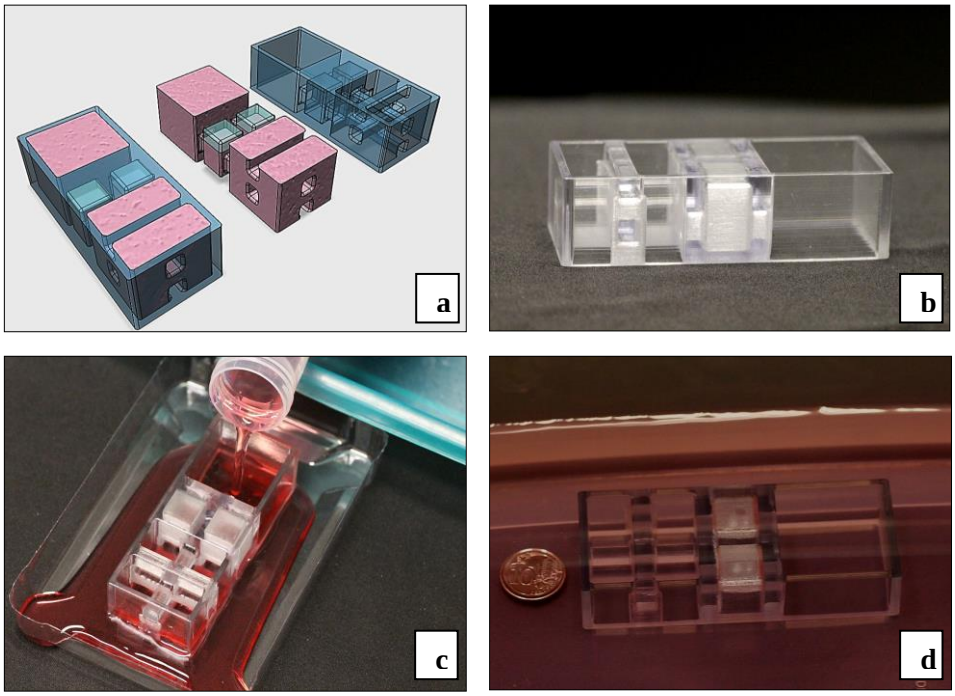

Fig. 7. Proof of concept for the air/oxygen trap design micromechanism based on optical evaluation of a flow simulation in the 25X scaled up functional prototype of the design mechanism; (a) from left to right: i) CAD model of the design micromechanism (blue transparent colour) designed for air/oxygen entrapment and visualization of the loading stem cell hydrogel (pink opaque colour), ii) visualization of the loading stem cell hydrogel (pink opaque colour) and the trapped air/oxygen at the top of each pore (green transparent boxes at the top of each pore), iii) CAD model of the mechanism , (b) side view of the 25X scaled up functional prototype of the design micromechanism, where are depicted the spatial configurations (design micromechanisms) designed to trap air/oxygen inside the pore (the design micromechanism consists of smaller inner space of the pores lower to the height of the interconnection canal compared to the inner space of the pores above the height of the interconnection canal), (c) cell growth media (red colour) was used for a flow simulation of the air/oxygen trap design micromechanism using the 25X scaled up functional prototype and (d) Photo taken following the fulfillment of the liquid carrier; scale bar (10 cents coin) and the cell media appears to fully cover the design micromechanism, while the top of the inner space of the pores appear with trapped air/oxygen bubbles (white areas at the top of each pore) following the infusion of the cell media through the 25X scaled up functional prototype (the media fully covered the prototype).

as a proof of concept evidence for the air/oxygen trap design micromechanism, as it verifies the design rational behind the "form-follows-function" design micromechanism, designed to trap air/oxygen at the top of each pore following the interaction of the innovative spatial configuration with the fluid forces.

The results of the experiment which appeared promising are analysed in the figure 7.

Therefore, similarly to the technology in microfluidics which develop systems able to provide air/oxygen at the top of each well in a cell culture plate (fig. 3), it appears with potential the entrapment of air/oxygen at the top of the pores of the graft following the infusion of the osteo-inductive hydrogel, developing so ability for oxygenation within the pores (artificial stem cell niches) of the graft.

7.5. Primary adipose derived stromal/stem cells plasticity

The differentiation potential of the primary adipose derived stromal cells so as to be used in future studies towards the further prototype to product development of the graft, was evaluated with imaging & histo-morphological analysis according to respective protocols of the three lineage differentiation test [114, 115]. In the 21st day of the culture, representative triplicates from the differentiation induction and non-differentiation induction groups (cell culture in 24-well tissue culture plates for the osteogenic/adipogenic groups and cell pellet culture for the chondrogenic lineage) were isolated, fixed and proceeded for staining, histological and immune-histochemical staining and imaging.

Relative to the morphological characteristics of the cells cultured in the 24-well tissue culture plates (fig. 8), the cells appeared with spindle cell shape in all groups and formation of lipid droplets in the differentiation group of the adipogenic lineage (fig. 8d and 8f). Relative to the staining results, the cells

appeared with moderate to strong alizarin red staining intensity towards the osteogenic direction (fig. 8b) and almost with no staining of the formed lipid droplets (fig. 8d) compared to the control groups (fig. 8a and 8c respectively) towards the adipogenic direction.

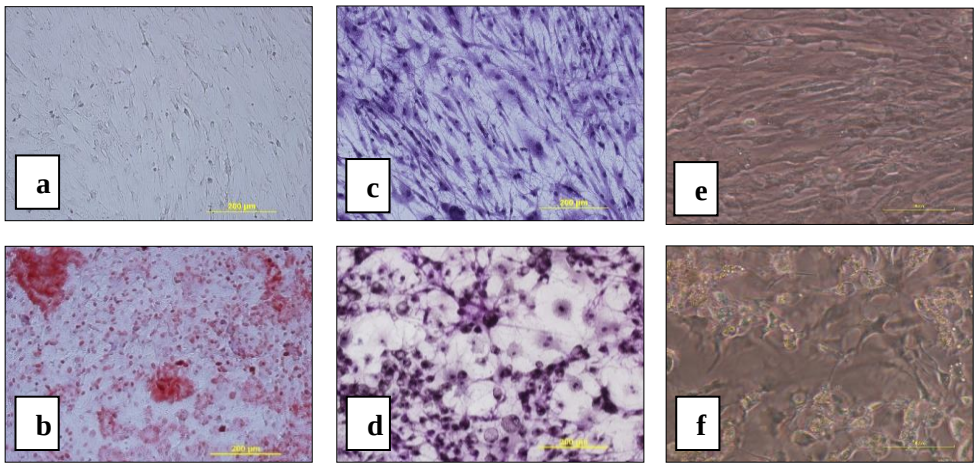

Fig. 8. Evaluation of the cells plasticity. Optical microscope photos for qualitative evaluation of the differentiation potential of adipose derived rabbit MSCs towards the osteogenic (a, b) and adipogenic direction (c,d,e,f) after 21 days of culture. Osteogenic direction; mineralization detection with moderate to strong alizarin red staining was observed in the differentiation group (b) compared to the control (a). Adipogenic direction; formation of cytoplasmic lipid droplets with fade oil red O staining (d) and without staining (f) was observed in the differentiation group compared to the control (c and e respectively). Magnification 20X. Scale bars: 200 um (a,b,c,d) and 100 um (e, f).

Relative to the staining results of the cells cultured in cell pellets (fig. 9), cells appeared with conflicting evidence as the immunohistochemical Col II staining appeared strong (fig. 9b) compared to the control group (fig. 9a), but the proteoglycan's safranin-O with fast green counter (fig. 9d) and the H&E staining for nucleus and cytoplasm (fig. 9f) appeared weak compared to the control groups (fig. 9c and 9e respectively). The above observations indicate a representative cellular phenotypic evidence of a mesenchymal stem cell (MSC) population for the adipose derived rabbit stromal cells with moderate differentiation ability.

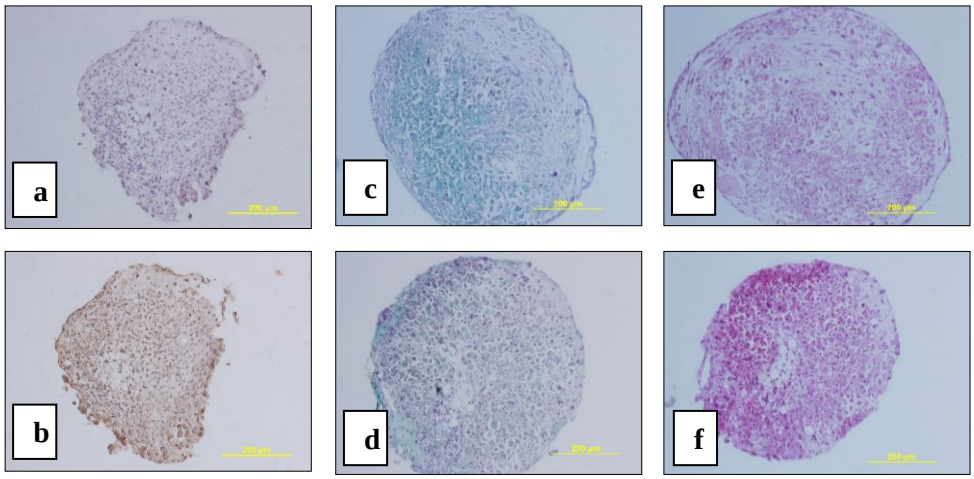

Fig. 9. Evaluation of the cells plasticity. Optical microscope photos for qualitative evaluation of the differentiation potential of adipose derived rabbit MSCs towards the chondrogenic direction after 21 days of culture; Strong brown immunohistochemical Col II staining was observed in the differentiation group (b) compared to the control (a). Fade red (red colour – green background) proteoglycan's safranin-O with fast green counter staining was observed in the differentiation group (d) compared to the control (c). More intense purplish blue and red H&E staining for cell's nucleus and cytoplasm respectively was observed in the differentiation group (f) compared to the control (e). Magnification 20X. Scale bar: 200um.

More particularly, relative to the osteogenic induction result (fig. 8a and b) and the potential use of the isolated cells in future studies for the prototype to product development of the graft, the staining evidence suggest a relationship of the cells to osteogenic induction. But, the spindle-like shape of the cells which does not appear so sharp as to strongly indicate an "osteoblastic" morphology (a strong indication of the cellular phenotype of the osteoblasts is apparent) and, most importantly, the moderate to strong intensity of the alizarin red staining, appear as insufficient evidence to predict the final cellular state, confirming a strong osteogenic differentiation ability of the cells.

Therefore, drawing a conclusion towards the characterization of the cells and the use of them in future studies for the further prototype to product development of the graft, the cells as a relatively homogeneous MSCs

population with moderate differentiation ability can be used in future studies efficiently for the evaluation of the cell positioning on the graft, by tracking the cell positioning on the graft following the infusion of the cells on it. But for further use and the purpose of the evaluation of the regeneration potential of the graft, where a robust cell line is needed with verified high osteogenic potential, the cells previously must undergo some purification of the population using flow cytometry, which could provide a more homogeneous and robust population. Alternatively, some other more robust market cell line can be used.

8. Future studies

Overview

In principle, future design-driven optimization studies are needed to link grafts' microarchitecture and cell behavior, providing quantitative microarchitectural reasoning for the design of TE scaffolds/grafts [109]. More efforts are needed towards the parameterization [116] of these studies as to provide key structural criteria for the design of the microarchitecture of a TE scaffold/graft. Co-axial studies with the current study on the computational microarchitecture design and the printing of a graft with more than one type of printing materials, may target as well programmable bilayer scaffolding microarchitecture patterns in space and time (4D printing) [117].

Considering as well the incremental nature of the scientific progress especially towards the development of novel "from scratch" research projects

like the current study, this study additionally isolates a primary adipose-derived stromal/stem cell population and suggests a further developmental pipeline, creating a complete design platform towards the future prototype to product development of the graft.

In particular, this study suggests the following detailed experimental setup for the continuation of the development of the graft:

Methods

Biomechanical evaluation of the scaffold (degradation, rheological properties and hydrophilicity): When the functional prototype will be printed, an evaluation protocol for the degradation rate [38], rheological properties [81] and the hydrophilicity [118] of the graft is suggested.

Tracking cell positioning - seeding efficiency: The evaluation of the seeding efficiency (cell numbers and distribution throughout the scaffolds) is been suggested by using qualitative manual histological [37] and automated image analysis with ImageJ software program based on the fluorescence intensity (mean relative fluorescence intensity - RFI) of each sample group, on images taken by semi-automated microscopy following eGFP transduction of the seeded cells [37].

Evaluation of oxygen supply: EPR oximetry is been suggested for the direct measurement of tissue pO2 [119].

In vitro evaluation of the osteogenic capacity of the scaffold: A combination of protocols which include the cck8, alizarin red and ALP

activity tests [81, 120] is been suggested for the in vitro evaluation of the cytocompatibility and osteogenicity.

Evaluation of vascularization: The quantified assessment of newly formed vessels on the graft is been suggested using eosin counterstained cryocuts and subsequent histomorphological imaging and analysis according to respective protocol [37].

In vivo evaluation of the osteogenic capacity of the scaffold: According to in vivo protocols from respective studies [39, 121], four groups of rabbit animal model is been suggested as to evaluate the in-vivo regeneration capacity of the graft, as following (the groups):

1. Untreated defect.
2. Scaffold-only treated.
3. Scaffold infused with stem cells.
4. Commercial available product.

More particularly, the selection of the commercial available product can be decided in a later time as a more advanced product might be launched in the market in the near future. In total, 4 groups is suggested (6 animals will represent each group, so the IACUC protocol will include 24 rabbits). According to the degradation rate of the PLGC block copolymer which is a material that is been suggested from the current study as the basis of the printing material for the further development of the graft (in the literature, the biodegradation rate of the PLGC appears to match the bone regeneration rate of up to 12 weeks), the rabbits can be sacrificed after 12 weeks. A combination of respective protocols [41, 121] for histological,

histomorphometrical and molecular analyses of the fracture healing is suggested.

Relative to the engraftment procedure, following adjustments in a suggested respective protocol [121], in rabbits' femoral bones from six animals of the groups 2 and 3, cylindrical scaffolds with (approximately) diameter of 2 cm and thickness of 1 cm can be implanted for about 12 weeks. It is expected that the graft will degrade mainly by hydrolysis while bone regeneration and biomineralization process gradually progresses (creeping substitution). The expected graft swelling following the implantation of the graft will be a desirable result as it will provide an adequate press fit between bone graft and host bone tissue.

Materials

Relative to the 3D printing materials, it is strongly suggested the prototype to product development of the graft and the respective 3D printing of the functional prototype and final model/graft, to be continued with an open extrusion/jet 3D printing system (e.g. RegenHU Bioprinter Biofactory), using as a basic printing material (following tests) an optimized mixture of the FDA approved biodegradable PLGC block copolymer (PLLA-co-PGA-co-PCL), the degradation rate of which has been tailored to match the bone regeneration rate of up to 12 weeks [25, 122] and Pluronic F127 as supporting sacrificial material [39]. The increase of the quantity of PCL in the mixture as to enhance the printability of the ink can be considered [123, 124], as PCL is a flexible TE material for standalone biofabrication and subsequent coating surface like

chitosan [125], as well for the development of composite materials with other synthetic [126] or natural [127] TE materials. Highly importantly PCL appears with properties that makes it one of the most suitable materials for 3D printing; low melting temperature (60 °C) and rapid cooling after extrusion [39]. Highly importantly also, when PCL is used as a printing material, no physicochemical changes to the PCL are expected caused by the printing-jetting process [128]. The mixture of hydroxyapatite (HA) in the PLGC copolymer can be also considered, as its addition is expected to increase the printability and the mechanical properties of the graft [129, 130], as well, its osteoconductive properties will provide a substrate for the stem cells to adhere and differentiate (the mechanotransduction pathway appears critical for MSCs differentiation to the osteoblastic lineage) [29]. In case that finally a RegenHU printer will be used for the 3D printing of the functional prototype and the final model/product, the osteoconductivity of the graft can also be enhanced with the mixture of the "osteoink" printing material in the above copolymer, which is a standardized commercial osteoconductive material provided from RegenHU.

Relative to the stem cell hydrogel, physically crosslinked hydrogels that gel spontaneously under physiological conditions in the temperature of the human body [131], they are suggested to constitute the basis for the development of the 2 microfluidics' composite hydrogels. Various cell numbers and concentrations of each component can be tested for the development of the composite hydrogels, mainly consisted of gelatin, fibrinogen, hyaluronic acid (HyA) and glycerol mixed into DMEM (high

glucose). This composite has already tested in previous studies and a good indication of the optimum cell density is been provided [15]. Further optimization of the flow rate, the dispensing uniformity, the mechanical properties (before and after cross-linking with thrombin) and the cell viability will be required. For the 1st microfluidics network (osteo-inductive network), the respective hydrogel is suggested to be incorporated with MSCs. For the 2nd microfluidics network (vascular-inductive network), the respective hydrogel is suggested to be incorporated with VEGF, MSCs, heparin and endothelial cells [90, 132-135].

Avoid pitfall strategy

The experimental design of this study as well of the subsequent suggested studies for the prototype to product development of the graft, frame a single-input multiple-output clear investigation plan of five independent objectives, in the strict context where the effects of the integrated geometrical parameters of the graft are not mixed with each other. The objectives have been classified and aligned to a five grade hierarchical diversification climax, based on increased manufacturing complexity/difficulty. The above setting provides the adequate flexibility in the implementation of future studies, as it allows the possibility to decrease the number of the objectives without affecting the integrity and novelty of the project.

9. Assumptions

A significant amount of evidence [29, 136-138] indicates that mechanical environment (mechanical loading type and magnitude) affects bone regeneration. So, as to avoid a multivariable experimental approach in the current study at the prototyping stage, the generated strain mechanical forces will be considered as experimental constant and the future prototype to product development studies may proceed as well in this way.

I mention here that in this direction and as mentioned at the beginning of this study, the manufacturing "friendly" approach to print the graft with a non cell-laden hydrogel, so as the biofunctionalization of the graft with the stem cells to occur following the manual injection of the graft with the stem cells, it is expected to provide rigidity to the final model/graft, as the frame-added construct would be more effective for supporting its original printed shape than a construct containing only cell-laden hydrogel.

10. Commercialization

The 2nd objective of the study has a clear commercial orientation as it targets the large scale personalized biofabrication of the graft.

11. Conclusion

New integrated design-driven optimization approaches not hindered by the limited capabilities of 3D printing technology may be needed to enhance translational impact in the research field of 3D printing Tissue Engineering.

In this context, by developing the prototype of an integrated 3D printed stem cell orthopedic graft according to a clear research plan where the effects of the geometrical parameters of the graft are not mixed with each other, this novel study argues the value of the integrated design-driven optimization perspective, triggering the development of a toolkit of microarchitecture-performance relations designed to tailor the large scale personalised biofabrication ability and regeneration capacity of the graft. The integrated design of the graft consists of a bio-inspired scaffolding microarchitecture and concurrently "form-follows-function" design micromechanisms in the design/manufacturing interface of 3D printing and microfluidics engineering.

Additionally, this study isolates a primary adipose-derived stromal/stem cell population and suggests a further developmental pipeline, creating a complete design platform towards the future prototype to product development of the graft.

12. Bibliography

1. Bertassoni, L.E. and P.G. Coelho, *Preface: engineering mineralized and load-bearing tissues: progress and challenges.* Adv Exp Med Biol, 2015. **881**: p. v-vii.
2. Fillingham, Y. and J. Jacobs, *Bone grafts and their substitutes.* Bone Joint J, 2016. **98-b**(1 Suppl A): p. 6-9.
3. Bell, A., D. Templeman, and J.C. Weinlein, *Nonunion of the Femur and Tibia: An Update.* Orthop Clin North Am, 2016. **47**(2): p. 365-75.
4. Fong, K., et al., *Predictors of nonunion and reoperation in patients with fractures of the tibia: an observational study.* BMC Musculoskelet Disord, 2013. **14**: p. 103.
5. Roberts, T.T. and A.J. Rosenbaum, *Bone grafts, bone substitutes and orthobiologics.* Organogenesis, 2012. **8**(4): p. 114-124.
6. Park, D., et al., *Chapter 7 - The Skeletal Stem Cell*, in *Osteoporosis (Fourth Edition)*. 2013, Academic Press: San Diego. p. 127-147.
7. Karsenty, G., *Transcriptional Control of Skeletogenesis.* Annual Review of Genomics and Human Genetics, 2008. **9**(1): p. 183-196.
8. Saeed, H., et al., *Mesenchymal stem cells (MSCs) as skeletal therapeutics-an update.* J Biomed Sci, 2016. **23**(1): p. 41.
9. Wu, M., G. Chen, and Y.-P. Li, *TGF-β and BMP signaling in osteoblast, skeletal development, and bone formation, homeostasis and disease.* Bone Research, 2016. **4**: p. 16009.

10. Lane, S.W., D.A. Williams, and F.M. Watt, *Modulating the stem cell niche for tissue regeneration.* Nat Biotechnol, 2014. **32**(8): p. 795-803.
11. Gomez-Barrena, E., et al., *Bone fracture healing: cell therapy in delayed unions and nonunions.* Bone, 2015. **70**: p. 93-101.
12. Tevlin, R., et al., *Stem and progenitor cells: advancing bone tissue engineering.* Drug Delivery and Translational Research, 2015. **6**(2): p. 159-173.
13. Grayson, W.L., et al., *Stromal cells and stem cells in clinical bone regeneration.* Nat Rev Endocrinol, 2015. **11**(3): p. 140-150.
14. Li, R., et al., *Endothelial progenitor cells for fracture healing: a microcomputed tomography and biomechanical analysis.* J Orthop Trauma, 2011. **25**(8): p. 467-71.
15. Tollemar, V., et al., *Stem cells, growth factors and scaffolds in craniofacial regenerative medicine.* Genes Dis, 2016. **3**(1): p. 56-71.
16. Hughes, D. and B. Song, *Dental and Nondental Stem Cell Based Regeneration of the Craniofacial Region: A Tissue Based Approach.* Stem Cells Int, 2016. **2016**: p. 8307195.
17. Maruyama, T., et al., *Stem cells of the suture mesenchyme in craniofacial bone development, repair and regeneration.* Nat Commun, 2016. **7**.
18. Watson, L., S.J. Elliman, and C.M. Coleman, *From isolation to implantation: a concise review of mesenchymal stem cell therapy in bone fracture repair.* Stem Cell Res Ther, 2014. **5**(2): p. 51.

19. Liu, Y., et al., *Therapeutic application of mesenchymal stem cells in bone and joint diseases.* Clin Exp Med, 2014. **14**(1): p. 13-24.

20. Kiernan, J., et al., *Systemic Mesenchymal Stromal Cell Transplantation Prevents Functional Bone Loss in a Mouse Model of Age-Related Osteoporosis.* Stem Cells Transl Med, 2016. **5**(5): p. 683-93.

21. Tawonsawatruk, T., et al., *Adipose derived pericytes rescue fractures from a failure of healing – non-union.* Scientific Reports, 2016. **6**: p. 22779.

22. Wang, P., et al., *Bone tissue engineering via human induced pluripotent, umbilical cord and bone marrow mesenchymal stem cells in rat cranium.* Acta Biomater, 2015. **18**: p. 236-48.

23. Zou, L., et al., *Angiogenic activity mediates bone repair from human pluripotent stem cell-derived osteogenic cells.* Scientific Reports, 2016. **6**: p. 22868.

24. De Coppi, P., et al., *Isolation of amniotic stem cell lines with potential for therapy.* Nat Biotechnol, 2007. **25**(1): p. 100-6.

25. Yeon Kwon, D., et al., *A computer-designed scaffold for bone regeneration within cranial defect using human dental pulp stem cells.* Scientific Reports, 2015. **5**: p. 12721.

26. Wu, G., et al., *Osteogenesis of peripheral blood mesenchymal stem cells in self assembling peptide nanofiber for healing critical size calvarial bony defect.* Scientific Reports, 2015. **5**: p. 16681.

27. Wan, C., Q. He, and G. Li, *Allogenic peripheral blood derived mesenchymal stem cells (MSCs) enhance bone regeneration in rabbit*

ulna critical-sized bone defect model. J Orthop Res, 2006. **24**(4): p. 610-8.

28. De Francesco, F., et al., *Human Adipose Stem Cells: From Bench to Bedside.* Tissue Eng Part B Rev, 2015. **21**(6): p. 572-84.
29. Trumbull, A., G. Subramanian, and E. Yildirim-Ayan, *Mechanoresponsive musculoskeletal tissue differentiation of adipose-derived stem cells.* Biomed Eng Online, 2016. **15**(1): p. 43.
30. Fisher, J.N., G.M. Peretti, and C. Scotti, *Stem Cells for Bone Regeneration: From Cell-Based Therapies to Decellularised Engineered Extracellular Matrices.* Stem Cells Int, 2016. **2016**: p. 9352598.
31. Zhang, X., et al., *Runx2-Modified Adipose-Derived Stem Cells Promote Tendon Graft Integration in Anterior Cruciate Ligament Reconstruction.* Scientific Reports, 2016. **6**: p. 19073.
32. Zlotnicki, J.P., et al., *Current State for Clinical Use of Stem Cells and Platelet-Rich Plasma.* Operative Techniques in Orthopaedics.
33. Smith, B.D. and D.A. Grande, *The current state of scaffolds for musculoskeletal regenerative applications.* Nat Rev Rheumatol, 2015. **11**(4): p. 213-22.
34. Jeon, O.H. and J. Elisseeff, *Orthopedic tissue regeneration: cells, scaffolds, and small molecules.* Drug Delivery and Translational Research, 2015. **6**(2): p. 105-120.
35. Guo, B., et al., *Functionalized scaffolds to enhance tissue regeneration.* Regen Biomater, 2015. **2**(1): p. 47-57.

36. Wüst, S., R. Müller, and S. Hofmann, *Controlled Positioning of Cells in Biomaterials—Approaches Towards 3D Tissue Printing.* Journal of Functional Biomaterials, 2011. **2**(3): p. 119.

37. Polzer, H., et al., *Comparison of Different Strategies for In Vivo Seeding of Prevascularized Scaffolds.* Tissue Engineering Part C: Methods, 2013. **20**(1): p. 11-18.

38. Shen, H., et al., *A biomimetic 3D microtubule-orientated poly(lactide-co-glycolide) scaffold with interconnected pores for tissue engineering.* Journal of Materials Chemistry B, 2015. **3**(21): p. 4417-4425.

39. Kang, H.-W., et al., *A 3D bioprinting system to produce human-scale tissue constructs with structural integrity.* Nat Biotech, 2016. **34**(3): p. 312-319.

40. Marenzana, M. and T.R. Arnett, *The Key Role of the Blood Supply to Bone.* Bone Res, 2013. **1**(3): p. 203-15.

41. Lu, C., et al., *The role of oxygen during fracture healing.* Bone, 2013. **52**(1): p. 220-229.

42. Zadpoor, A.A., *Bone tissue regeneration: the role of scaffold geometry.* Biomaterials Science, 2015. **3**(2): p. 231-245.

43. Murphy, S.V. and A. Atala, *3D bioprinting of tissues and organs.* Nat Biotech, 2014. **32**(8): p. 773-785.

44. Shafiee, A. and A. Atala, *Printing Technologies for Medical Applications.* Trends in Molecular Medicine, 2016. **22**(3): p. 254-265.

45. Do, A.V., et al., *3D Printing of Scaffolds for Tissue Regeneration Applications.* Adv Healthc Mater, 2015. **4**(12): p. 1742-62.

46. Mandrycky, C., et al., *3D bioprinting for engineering complex tissues.* Biotechnol Adv, 2015.

47. Scadden, D. and A. Srivastava, *Advancing Stem Cell Biology toward Stem Cell Therapeutics.* Cell Stem Cell, 2012. **10**(2): p. 149-150.

48. Fernandez-Yague, M.A., et al., *Biomimetic approaches in bone tissue engineering: Integrating biological and physicomechanical strategies.* Advanced Drug Delivery Reviews, 2015. **84**: p. 1-29.

49. Tang, D., et al., *Biofabrication of bone tissue: approaches, challenges and translation for bone regeneration.* Biomaterials, 2016. **83**: p. 363-382.

50. Uygun, B.E., M.L. Yarmush, and K. Uygun, *Application of whole-organ tissue engineering in hepatology.* Nat Rev Gastroenterol Hepatol, 2012. **9**(12): p. 738-744.

51. Derby, B., *Printing and prototyping of tissues and scaffolds.* Science, 2012. **338**(6109): p. 921-6.

52. Johnson, B.N., et al., *3D Printed Anatomical Nerve Regeneration Pathways.* Adv Funct Mater, 2015. **25**(39): p. 6205-6217.

53. Cui, H., et al., *Biologically Inspired Smart Release System Based on 3D Bioprinted Perfused Scaffold for Vascularized Tissue Regeneration.* Advanced Science, 2016: p. n/a-n/a.

54. Yuen, W.W., et al., *Mimicking nature by codelivery of stimulant and inhibitor to create temporally stable and spatially restricted angiogenic zones.* Proceedings of the National Academy of Sciences, 2010. **107**(42): p. 17933-17938.

55. Gariboldi, M.I. and S.M. Best, *Effect of Ceramic Scaffold Architectural Parameters on Biological Response.* Front Bioeng Biotechnol, 2015. **3**: p. 151.

56. Sun, W., et al., *Bio-CAD modeling and its applications in computer-aided tissue engineering.* Computer-Aided Design, 2005. **37**(11): p. 1097-1114.

57. Loh, Q.L. and C. Choong, *Three-dimensional scaffolds for tissue engineering applications: role of porosity and pore size.* Tissue Eng Part B Rev, 2013. **19**(6): p. 485-502.

58. Matsiko, A., J.P. Gleeson, and F.J. O'Brien, *Scaffold Mean Pore Size Influences Mesenchymal Stem Cell Chondrogenic Differentiation and Matrix Deposition.* Tissue Engineering Part A, 2014. **21**(3-4): p. 486-497.

59. Duan, P., et al., *The effects of pore size in bilayered poly(lactide-co-glycolide) scaffolds on restoring osteochondral defects in rabbits.* Journal of Biomedical Materials Research Part A, 2014. **102**(1): p. 180-192.

60. Saito, E., et al., *Effects of designed PLLA and 50:50 PLGA scaffold architectures on bone formation in vivo.* J Tissue Eng Regen Med, 2013. **7**(2): p. 99-111.

61. Boccaccio, A., et al., *Geometry Design Optimization of Functionally Graded Scaffolds for Bone Tissue Engineering: A Mechanobiological Approach.* PLoS One, 2016. **11**(1): p. e0146935.

62. Tien, J., *Microfluidic approaches for engineering vasculature.* Current Opinion in Chemical Engineering, 2014. **3**: p. 36-41.

63. Hasan, A., et al., *Microfluidic techniques for development of 3D vascularized tissue.* Biomaterials, 2014. **35**(26): p. 7308-25.

64. Giannitelli, S.M., et al., *Current trends in the design of scaffolds for computer-aided tissue engineering.* Acta Biomater, 2014. **10**(2): p. 580-94.

65. Yoo, D.-J., *Recent trends and challenges in computer-aided design of additive manufacturing-based biomimetic scaffolds and bioartificial organs.* International Journal of Precision Engineering and Manufacturing, 2014. **15**(10): p. 2205-2217.

66. Mota, C., et al., *Additive manufacturing techniques for the production of tissue engineering constructs.* J Tissue Eng Regen Med, 2015. **9**(3): p. 174-90.

67. Wust, S., R. Muller, and S. Hofmann, *3D Bioprinting of complex channels-Effects of material, orientation, geometry, and cell embedding.* J Biomed Mater Res A, 2015. **103**(8): p. 2558-70.

68. Ozbolat, I.T., *Bioprinting scale-up tissue and organ constructs for transplantation.* Trends in Biotechnology, 2015. **33**(7): p. 395-400.

69. Raney, J.R. and J.A. Lewis, *Printing mesoscale architectures.* MRS Bulletin, 2015. **40**(11): p. 943-950.

70. Duro-Royo, J., L. Mogas-Soldevila, and N. Oxman, *Flow-based fabrication: An integrated computational workflow for design and*

digital additive manufacturing of multifunctional heterogeneously structured objects. Computer-Aided Design, 2015. **69**: p. 143-154.

71. Studart, A.R., *Biological and Bioinspired Composites with Spatially Tunable Heterogeneous Architectures.* Advanced Functional Materials, 2013. **23**(36): p. 4423-4436.

72. Zopf, D.A., et al., *Computer aided-designed, 3-dimensionally printed porous tissue bioscaffolds for craniofacial soft tissue reconstruction.* Otolaryngol Head Neck Surg, 2015. **152**(1): p. 57-62.

73. Sobral, J.M., et al., *Three-dimensional plotted scaffolds with controlled pore size gradients: Effect of scaffold geometry on mechanical performance and cell seeding efficiency.* Acta Biomater, 2011. **7**(3): p. 1009-18.

74. Melchels, F.P.W., et al., *Effects of the architecture of tissue engineering scaffolds on cell seeding and culturing.* Acta Biomaterialia, 2010. **6**(11): p. 4208-4217.

75. Reed, S., et al., *Macro- and micro-designed chitosan-alginate scaffold architecture by three-dimensional printing and directional freezing*. Biofabrication, 2016. **8**(1).

76. Melchels, F.P.W., et al., *The influence of the scaffold design on the distribution of adhering cells after perfusion cell seeding.* Biomaterials, 2011. **32**(11): p. 2878-2884.

77. Yang, N., Y. Tian, and D. Zhang, *Novel real function based method to construct heterogeneous porous scaffolds and additive manufacturing*

for use in medical engineering. Medical Engineering & Physics, 2015. **37**(11): p. 1037-1046.

78. Guyot, Y., et al., *A computational model for cell/ECM growth on 3D surfaces using the level set method: a bone tissue engineering case study.* Biomech Model Mechanobiol, 2014. **13**(6): p. 1361-71.
79. Liu, A., et al., *3D Printing Surgical Implants at the clinic: A Experimental Study on Anterior Cruciate Ligament Reconstruction.* Scientific Reports, 2016. **6**: p. 21704.
80. Jung, J.W., J.-S. Lee, and D.-W. Cho, *Computer-aided multiple-head 3D printing system for printing of heterogeneous organ/tissue constructs.* Scientific Reports, 2016. **6**: p. 21685.
81. Pati, F., et al., *Printing three-dimensional tissue analogues with decellularized extracellular matrix bioink.* Nat Commun, 2014. **5**.
82. Studart, A.R., *Additive manufacturing of biologically-inspired materials.* Chemical Society Reviews, 2016. **45**(2): p. 359-376.
83. Chelsea, M.M., L.A. Daniel, and S.A. Kristi, *Bio-inspired 3D microenvironments: a new dimension in tissue engineering.* Biomedical Materials, 2016. **11**(2): p. 022001.
84. Wegst, U.G.K., et al., *Bioinspired structural materials.* Nat Mater, 2015. **14**(1): p. 23-36.
85. Vunjak-Novakovic, G. and D.T. Scadden, *Biomimetic platforms for human stem cell research.* Cell Stem Cell, 2011. **8**(3): p. 252-61.

86. Rouwkema, J. and A. Khademhosseini, *Vascularization and Angiogenesis in Tissue Engineering: Beyond Creating Static Networks.* Trends in Biotechnology.

87. Hutton, D.L. and W.L. Grayson, *Stem cell-based approaches to engineering vascularized bone.* Current Opinion in Chemical Engineering, 2014. **3**: p. 75-82.

88. Lindhorst, D., et al., *Effects of VEGF loading on scaffold-confined vascularization.* Journal of Biomedical Materials Research Part A, 2010. **95A**(3): p. 783-792.

89. Keith, B. and M.C. Simon, *Hypoxia-inducible factors, stem cells, and cancer.* Cell, 2007. **129**(3): p. 465-72.

90. Jin, K., et al., *In vivo vascularization of MSC-loaded porous hydroxyapatite constructs coated with VEGF-functionalized collagen/heparin multilayers.* Sci Rep, 2016. **6**: p. 19871.

91. Nauta, T.D., V.W.M. van Hinsbergh, and P. Koolwijk, *Hypoxic Signaling During Tissue Repair and Regenerative Medicine.* International Journal of Molecular Sciences, 2014. **15**(11): p. 19791-19815.

92. Fernandez, C.E., et al., *Biological and engineering design considerations for vascular tissue engineered blood vessels (TEBVs).* Current Opinion in Chemical Engineering, 2014. **3**: p. 83-90.

93. Samorezov, J.E. and E. Alsberg, *Spatial regulation of controlled bioactive factor delivery for bone tissue engineering.* Advanced Drug Delivery Reviews, 2015. **84**: p. 45-67.

94. Kim, C., et al., *3-Dimensional cell culture for on-chip differentiation of stem cells in embryoid body*. Lab Chip, 2011. **11**(5): p. 874-82.

95. Polzer, H., et al., *Long-term detection of fluorescently labeled human mesenchymal stem cell in vitro and in vivo by semi-automated microscopy*. Tissue Eng Part C Methods, 2012. **18**(2): p. 156-65.

96. Sart, S., T. Ma, and Y. Li, *Preconditioning stem cells for in vivo delivery*. Biores Open Access, 2014. **3**(4): p. 137-49.

97. Sart, S., et al., *Three-dimensional aggregates of mesenchymal stem cells: cellular mechanisms, biological properties, and applications.* Tissue Eng Part B Rev, 2014. **20**(5): p. 365-80.

98. Lo, Y.-P., et al., *Three-dimensional spherical spatial boundary conditions differentially regulate osteogenic differentiation of mesenchymal stromal cells.* Scientific Reports, 2016. **6**: p. 21253.

99. Lou, Y.R., et al., *Silica bioreplication preserves three-dimensional spheroid structures of human pluripotent stem cells and HepG2 cells.* Sci Rep, 2015. **5**: p. 13635.

100. Huebsch, N., et al., *Miniaturized iPS-Cell-Derived Cardiac Muscles for Physiologically Relevant Drug Response Analyses.* Scientific Reports, 2016. **6**: p. 24726.

101. Cheng, N.C., S. Wang, and T.H. Young, *The influence of spheroid formation of human adipose-derived stem cells on chitosan films on stemness and differentiation capabilities.* Biomaterials, 2012. **33**(6): p. 1748-58.

102. Bhattacharjee, N., et al., *The upcoming 3D-printing revolution in microfluidics.* Lab on a Chip, 2016. **16**(10): p. 1720-1742.

103. Kronenberg, H.M., *Developmental regulation of the growth plate.* Nature, 2003. **423**(6937): p. 332-6.

104. Ma, T., et al., *Hypoxia and stem cell-based engineering of mesenchymal tissues.* Biotechnol Prog, 2009. **25**(1): p. 32-42.

105. Levenberg, S., et al., *Engineering vascularized skeletal muscle tissue.* Nat Biotechnol, 2005. **23**(7): p. 879-84.

106. Woo Jung, J., et al., *Evaluation of the Effective Diffusivity of a Freeform Fabricated Scaffold Using Computational Simulation.* Journal of Biomechanical Engineering, 2013. **135**(8): p. 084501-084501.

107. Agarwal, P., et al., *A Biomimetic Core-Shell Platform for Miniaturized 3D Cell and Tissue Engineering.* Part Part Syst Charact, 2015. **32**(8): p. 809-816.

108. Velasco, M.A., C.A. Narvaez-Tovar, and D.A. Garzon-Alvarado, *Design, materials, and mechanobiology of biodegradable scaffolds for bone tissue engineering.* Biomed Res Int, 2015. **2015**: p. 729076.

109. Ashworth, J.C., S.M. Best, and R.E. Cameron, *Quantitative architectural description of tissue engineering scaffolds.* Materials Technology, 2014. **29**(5): p. 281-295.

110. Brennan, M.D., M.L. Rexius-Hall, and D.T. Eddington, *A 3D-Printed Oxygen Control Insert for a 24-Well Plate.* PLoS One, 2015. **10**(9): p. e0137631.

111. Liu, J., et al., *Direct 3D-printing of cell-laden constructs in microfluidic architectures.* Lab on a Chip, 2016. **16**(8): p. 1430-1438.

112. Pan, T., et al., *3D Bioplotting of Gelatin/Alginate Scaffolds for Tissue Engineering: Influence of Crosslinking Degree and Pore Architecture on Physicochemical Properties.* Journal of Materials Science & Technology.

113. Dubois, S.G., et al., *Isolation of human adipose-derived stem cells from biopsies and liposuction specimens.* Methods Mol Biol, 2008. **449**: p. 69-79.

114. Yang, Z., J.F. Schmitt, and E.H. Lee, *Immunohistochemical analysis of human mesenchymal stem cells differentiating into chondrogenic, osteogenic, and adipogenic lineages.* Methods Mol Biol, 2011. **698**: p. 353-66.

115. See, E.Y., S.L. Toh, and J.C. Goh, *Multilineage potential of bone-marrow-derived mesenchymal stem cell cell sheets: implications for tissue engineering.* Tissue Eng Part A, 2010. **16**(4): p. 1421-31.

116. Ashworth, J.C., et al., *Parameterizing the Transport Pathways for Cell Invasion in Complex Scaffold Architectures.* Tissue Eng Part C Methods, 2016. **22**(5): p. 409-17.

117. Sydney Gladman, A., et al., *Biomimetic 4D printing.* Nat Mater, 2016. **15**(4): p. 413-8.

118. Yang, Z., et al., *Improved Mesenchymal Stem Cells Attachment and In Vitro Cartilage Tissue Formation on Chitosan-Modified Poly(l-*

Lactide-co-Epsilon-Caprolactone) Scaffold. Tissue Engineering Part A, 2011. **18**(3-4): p. 242-251.

119. Khan, N., et al., *Repetitive tissue pO2 measurements by electron paramagnetic resonance oximetry: current status and future potential for experimental and clinical studies.* Antioxid Redox Signal, 2007. **9**(8): p. 1169-82.

120. Tan, S.L., et al., *Isolation, characterization and the multi-lineage differentiation potential of rabbit bone marrow-derived mesenchymal stem cells.* J Anat, 2013. **222**(4): p. 437-50.

121. Li, C., et al., *Biocompatibility and in vivo osteogenic capability of novel bone tissue engineering scaffold A-W-MGC/CS.* J Orthop Surg Res, 2014. **9**: p. 100.

122. Kwon, D.Y., et al., *Preparation of three-dimensional scaffolds by using solid freeform fabrication and feasibility study of the scaffolds.* Journal of Materials Chemistry B, 2014. **2**(12): p. 1689-1698.

123. Kundu, J., et al., *An additive manufacturing-based PCL-alginate-chondrocyte bioprinted scaffold for cartilage tissue engineering.* J Tissue Eng Regen Med, 2015. **9**(11): p. 1286-97.

124. Temple, J.P., et al., *Engineering anatomically shaped vascularized bone grafts with hASCs and 3D-printed PCL scaffolds.* J Biomed Mater Res A, 2014. **102**(12): p. 4317-25.

125. Zhang, T., et al., *Cross-talk between TGF-beta/SMAD and integrin signaling pathways in regulating hypertrophy of mesenchymal stem*

cell chondrogenesis under deferral dynamic compression. Biomaterials, 2015. **38**: p. 72-85.

126. Rai, B., et al., *Differences between in vitro viability and differentiation and in vivo bone-forming efficacy of human mesenchymal stem cells cultured on PCL-TCP scaffolds.* Biomaterials, 2010. **31**(31): p. 7960-70.

127. Ekaputra, A.K., et al., *Composite electrospun scaffolds for engineering tubular bone grafts.* Tissue Eng Part A, 2009. **15**(12): p. 3779-88.

128. Li, J.L., et al., *Fabrication of three-dimensional porous scaffolds with controlled filament orientation and large pore size via an improved E-jetting technique.* J Biomed Mater Res B Appl Biomater, 2014. **102**(4): p. 651-8.

129. Luo, Y., et al., *Concentrated gelatin/alginate composites for fabrication of predesigned scaffolds with a favorable cell response by 3D plotting.* RSC Advances, 2015. **5**(54): p. 43480-43488.

130. Gilchrist, C.L., et al., *Micro-scale and meso-scale architectural cues cooperate and compete to direct aligned tissue formation.* Biomaterials, 2014. **35**(38): p. 10015-24.

131. Van Tomme, S.R., G. Storm, and W.E. Hennink, *In situ gelling hydrogels for pharmaceutical and biomedical applications.* Int J Pharm, 2008. **355**(1-2): p. 1-18.

132. Pedersen, T.O., et al., *Mesenchymal stem cells induce endothelial cell quiescence and promote capillary formation.* Stem Cell Res Ther, 2014. **5**(1): p. 23.

133. Freiman, A., et al., *Adipose-derived endothelial and mesenchymal stem cells enhance vascular network formation on three-dimensional constructs in vitro.* Stem Cell Res Ther, 2016. **7**: p. 5.

134. Poh, C.K., et al., *The effect of VEGF functionalization of titanium on endothelial cells in vitro.* Biomaterials, 2010. **31**(7): p. 1578-85.

135. Shi, Z., et al., *Enhanced endothelial differentiation of adipose-derived stem cells by substrate nanotopography.* J Tissue Eng Regen Med, 2014. **8**(1): p. 50-8.

136. Yang, P.F., G.P. Bruggemann, and J. Rittweger, *What do we currently know from in vivo bone strain measurements in humans?* J Musculoskelet Neuronal Interact, 2011. **11**(1): p. 8-20.

137. Campàs, O., *A toolbox to explore the mechanics of living embryonic tissues.* Seminars in Cell & Developmental Biology.

138. Andrade-Campos, A.n., A.n. Ramos, and J.A. Sim?es, *A model of bone adaptation as a topology optimization process with contact.* Journal of Biomedical Science and Engineering, 2012. **Vol.05No.05**: p. 16.